Cadmium Stress Responses in Brassica juncea: Hints from Proteomics and Metabolomics

ARTICLE *in* JOURNAL OF PROTEOME RESEARCH · SEPTEMBER 2013

Impact Factor: 4.25 · DOI: 10.1021/pr400793e · Source: PubMed

Journal of proteome research

Article

pubs.acs.org/jpr

Cadmium Stress Responses in *Brassica juncea*: Hints from Proteomics and Metabolomics

Angelo D'Alessandro,[†,§] Manel Taamalli,[‡,§] Federica Gevi,[†] Anna Maria Timperio,[†] Lello Zolla,[*,†] and Tahar Ghnaya[*,‡]

[†]Department of Ecological and Biological Sciences, University of Tuscia, Largo dell'Università, snc, 01100 Viterbo, Italy

[‡]Laboratoire des Plantes Extrêmophiles, Centre de Biotechnologie de Borj-Cédria, BP 901, 2050 Hammam-lif, Tunisia

Supporting Information

ABSTRACT: Among heavy metal stressors, cadmium (Cd) pollution is one leading threat to the environment. In this view, research efforts have been increasingly put forward to promote the individuation of phytoextractor plants that are capable of accumulating and withstanding the toxic metals, including Cd, in the aerial parts. We hereby adopted the hyperaccumulator *B. juncea* (Indian mustard) as a model to investigate plant responses to Cd stress at low (25 μM) and high (100 μM) doses. Analytical strategies included mass-spectrometry-based determination of Cd and the assessment of its effect on the leaf proteome and metabolome. Results were thus integrated with routine physiological data. Taken together, physiology results highlighted the deregulation of photosynthesis efficiency, ATP synthesis, reduced transpiration, and the impairment of light-independent carbon fixation reactions. These results were supported at the proteomics level by the observed Cd-dependent alteration of photosystem components and the alteration of metabolic enzymes, including ATP synthase subunits, carbonic anhydrase, and enzymes involved in antioxidant responses (especially glutathione and phytochelatin homeostasis) and the Calvin cycle. Metabolomics results confirmed the alterations of energy-generating metabolic pathways, sulfur-compound metabolism (GSH and PCs), and Calvin cycle. Besides, metabolomics results highlighted the up-regulation of phosphoglycolate, a byproduct of the photorespiration metabolism. This was suggestive of the likely increased photorespiration rate as a means to cope with Cd-induced unbalance in stomatal conductance and deregulation of CO_2 homeostasis, which would, in turn, promote CO_2 depletion and O_2 (and thus oxidative stress) accumulation under prolonged photosynthesis in the leaves from plants exposed to high doses of $CdCl_2$. Overall, it emerges that Cd-stressed *B. juncea* might rely on photorespiration, an adaptation that would prevent the over-reduction of the photosynthetic electron transport chain and photoinhibition.

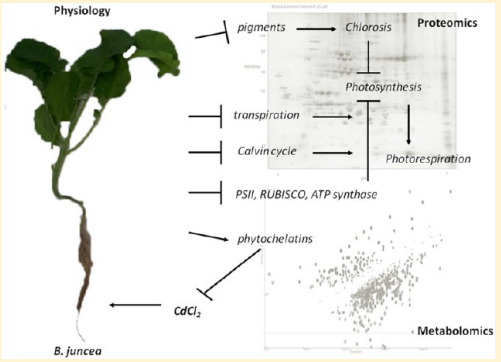

KEYWORDS: *Brassica juncea, cadmium chloride, bioremediation, abiotic stress responses, mass spectrometry*

1. INTRODUCTION

During the last decades, phytoremediation has emerged as an environmentally friendly and relatively cheap strategy to clean up heavy metals from contaminated soils, especially in comparison with traditional physicochemical remediation approaches.[1] This is relevant in light of the dramatic rise in the levels of heavy metal soil contamination during the late 19th and early 20th centuries.

Heavy-metal pollutants may be introduced into the environment by many anthropogenic activities, such as mining, use of chemical fertilizers or metal-based pesticides, and a wide range of industrial activities.[2] In particular, cadmium (Cd) is a widespread pollutant that often occurs in air and soils exposed to heavy traffic and industrial wastes (power stations, heating systems, metal-working industries, waste incinerators, and cement factories).

The main source of Cd exposure in the general population is through the food chain, whereby contaminated plants would represent the first step either in terms of direct human consumption or, indirectly, as a key aliment for bred animals.

A significant body of compelling evidence has been documented over the years suggesting that Cd induces multiple damages in every organism examined, including humans[3] and plants.[4] Therefore, the persistence and bioaccumulation of Cd and other metals, such as zinc (Zn), mercury (Hg), copper (Cu), arsenic (As), and lead (Pb), poses a threat in terms of toxicity to living organisms, from microorganisms to animals. From this viewpoint, it is worth noting that proteomics and Omics technologies have recently expanded the meaning of the statement "we are what we eat".[5]

In biological terms, Cd shares chemical similarity to Zn, Fe, and Ca and can thus replace them in the prosthetic group of many proteins.[6]

Special Issue: Agricultural and Environmental Proteomics

Received: August 1, 2013

dx.doi.org/10.1021/pr400793e | *J. Proteome Res.* XXXX, XXX, XXX–XXX

In the plant, Cd triggers a domino of molecular mechanisms, as it has been largely documented.[7−10] Cd can induce severe disturbances in the physiological processes of a plant, affecting vital functions such as photosynthesis, water relations, and mineral uptake.[7−12] Most evidently, Cd toxicity is accompanied by growth retardation, leaf chlorosis, and inhibition of diverse metabolic processes including photosynthesis, respiration, and assimilation of divalent ions. As far as photosynthesis is concerned, Cd promotes premature senescence of chloroplast, which is accompanied by stomatal closure, inhibition of carbon assimilation, and photosynthetic electron transport.[7−12] By inhibiting the synthesis of chlorophylls (Chl) and destabilizing their interaction with proteins by forming Cd−Chl complexes, Cd promotes the accumulation of pigment lipoprotein complexes, especially of photosystem I (PSI), and induces Fe-deficiency-like chlorosis in plants.[8]

Proteomic analyses by 2D BN-SDS-PAGE and mass spectrometry showed that Fe deficiency in Cd-stressed plants considerably decreased the amount of LHCII trimer, ATPase-F1 portion, cyt b6/f, and RuBisCO.[13,14] Cd-mediated prolonged inhibition of photosynthesis in Cd-sensitive plants triggers oxidative stress and reactive oxygen species (ROS)-mediated degradation of photosynthetic structures. Indeed, Cd promotes the generation of several ROS, such as the superoxide radical ($O_2^{\bullet-}$), hydrogen peroxide (H_2O_2), and the hydroxyl radical (HO•). Cd-generated ROS can accelerate membrane lipid peroxidation, which impairs cell membrane fluidity and permeability.[15] Plant defensive mechanisms to cope with oxidative stress involve transcriptional regulation of Cd-responsive genes, which results in the induction of antioxidant systems. Cadmium has a strong affinity for thiolates, which renders it toxic to the plant, as important enzymes are inactivated when Cd binds to sulfhydryl groups (−SH). In turn, plants exploit thiolated compounds, phytochelatins, to chelate Cd and mediate its assimilation, transport, and compartmentalization.[16,17]

Conversely, Cd has been shown to inhibit ROS-detoxifying enzymes such as superoxide dismutase (SOD) and ascorbate peroxidase. Defensive mechanisms also rely on cross talks between ROS-mediated signaling and plant hormones. Indeed, compelling evidence has been produced to underpin the hypothesis about a central role of plant hormones in the signaling responses of Cd-induced stress.[18−20]

In the light of the extreme phytotoxicity of Cd, only a few plant species are resistant enough to tolerate Cd, basically via two main strategy: the excluder strategy, in which the plants try to avoid heavy metals entering the roots, and the tolerant/accumulator strategy. In the latter case, the poisonous metal is accumulated in the aerial part, a pivotal requirement for "phytoextractor" plants for phytoremediation purposes.[21,22] Among the *Brassicaceae* family, some species such as *Brassica juncea* were appreciated as potential heavy metal-phytoextractor candidates as they are suitable for bioremediation purposes. It is thus a small wonder that during the last 25 years, Indian mustard (*B. juncea*) has represented a key model to investigate the mechanisms underlying adaptation responses to Cd stress and accumulation.[23−41]

The diffusion of Omics technologies, above all transcriptomics and proteomics, has paved the way for a deeper understanding of the molecular events driving plant responses to abiotic stresses and, in particular, *B. juncea* adaptation to prolonged Cd exposure.[42−44] However, further advancements in the phytoremediation research endeavor have been promoted by recent progresses in the field of metabolomics, resulting from the introduction of technological advancements in mass spectrometry and the availability of databases for post hoc data elaboration. In this view, we hereby performed an integrated proteomics and metabolomics approach to investigate the effects of Cd exposure in *B. juncea*, so as to confirm physiological data already available from the literature and expand them with the results obtained through the application of innovative analytical Omics strategies.

2. MATERIALS AND METHODS

Plant Growth Condition and Cd Treatment

Seeds of Indian mustard (*Brassica juncea*, accession no. 426308) identified as a metal accumulator[45] were obtained from the North Central Regional Plant Introduction Station (NCRPIS - United States Department of Agriculture (USDA) from United States of America - Ames, IA). Seeds of *B. juncea* were surface sterilized, germinated in Petri dishes (10 cm) containing two layers of filter papers moistened with deionized water, and incubated in the dark at 30 °C for 4 days. Following germination, seedlings were transferred to plastic pots filled with 5 L of nutrient solution containing 136 mg L^{-1} KH_2PO_4, 492.3 mg L^{-1} $Ca(NO3)_2$, 303 mg L^{-1} KNO_3, 17.4 mg L^{-1} K_2HPO_4, 146 mg L^{-1} $MgSO_4$, 1.98 mg L^{-1} $MnCl_2$, 0.294 mg L^{-1} $CuSO_4$, 0.287 mg L^{-1} $ZnSO_4$, 1.85 mg L^{-1} H_3BO_3, 0.37 mg L^{-1} $(NH_4)MoO_4$, and 20 μM Fe-EDTA (Hoagland and Arnon, 1950). The experiments were carried out in a greenhouse chamber with day/night temperature and humidity regime of 25/20 °C and 55/75% relative humidity (RH), respectively. A 16 h (daily) photoperiod was used. Growth solutions were continuously aerated and renewed every 3 days. After 2 weeks of Cd-free growth, seedlings were randomly assigned to four different Cd treatments: 0, 25, 50, and 100 μM $CdCl_2$ for duration of 21 days. At harvest, plants were divided into shoots and roots. Roots were immersed in cold distilled water and then gently blotted with filter-paper.

For biomass determination, after measurement of fresh weight, shoots and roots were oven-dried at 60 °C until they reached a constant weight.

Leaves used for proteomics and metabolomics analyses were immediately frozen in liquid nitrogen.

Cadmium Concentration and Physiological Parameters

Cd content in *B. juncea* shoots and roots was assayed via ICP MS, as previously reported.[45] Plant dry weight, nitrogen, potassium, magnesium and calcium content, pigments, and photosystem activity parameters were all assayed in agreement with our previous reports.[6,13,14,45]

Proteomics

Protein Extraction and 2DE. Leaves were finely ground in liquid nitrogen, and the protein extraction, 2DE protocol, and analysis were performed in agreement with Fagioni et al.[14] Proteins were stained by Coomassie Brilliant Blue G-250 stain. A total of 12 2DE gels (four biological replicates per group − control, 25 μM, and 100 μM $CdCl_2$) have been performed during the proteomic analysis. Stained gels were digitalized, and image analysis was performed using PDQuest 2-D analysis software 1709620 (Biorad, Milan, Italy).

Spots from 2-DE maps of biological interest ($p < 0.05$ ANOVA, fold-change ≥1.5) were carefully excised from the gel and subjected to in-gel trypsin digestion according to Shevchenko et al.[48] with minor modifications. Protein

dx.doi.org/10.1021/pr400793e | J. Proteome Res. XXXX, XXX, XXX−XXX

identification was performed as previously reported[49] through a nanoHPLC (Proxeon, Bruker Daltonics, Germany) and MS/MS ion trap (Amazon ETD, Bruker Daltonics) system. Instrument settings were consistent with our previous studies.[50] In particular, the spray capillary was a fused silica capillary, 0.090 mm o.d., 0.020 mm i.d. For all experiments, a sample volume of 15 μL was loaded by the autosampler onto a homemade 2 cm fused silica precolumn (100 μm I.D.; 375 μm o.d.; Reprosil C18-AQ, 5 μm, Dr. Maisch, Ammerbuch-Entringen, Germany). Sequential elution of peptides was accomplished using a flow rate of 300 nL/min and a linear gradient from Solution A (2% acetonitrile; 0.1% formic acid) to 50% of Solution B (98% acetonitrile; 0.1% formic acid) in 40 min over the precolumn in-line with a homemade 15 cm resolving column (75 μm i.d.; 375 μm o.d.; Reprosil C18-AQ, 3 μm, Dr. Maisch). The acquisition parameters for the instrument were as follows: dry gas temperature, 220 °C; dry gas, 4.0 L/min; nebulizer gas, 10 psi; electrospray voltage, 4000 V; high-voltage end-plate offset, −200 V; capillary exit, 140 V; trap drive: 63.2; funnel 1 in, 100 V out 35 V and funnel 2 in, 12 V out 10 V; ICC target, 200 000; maximum accumulation time, 50 ms. The sample was measured with the "Enhanced Resolution Mode" at 8100 m/z per second (which allows mono isotopic resolution up to four charge stages) polarity positive, scan range from m/z 300 to 1500, five spectra averaged, and rolling average of 1. The "Smart Decomposition" was set to "auto".

Acquired CID spectra were processed in DataAnalysis 4.0, and deconvoluted spectra were further analyzed with BioTools 3.2 software and submitted to Mascot search program (in-house version 2.2, Matrix Science, London, U.K.).

The following parameters were adopted for database searches with Mascot search program: NCBInr database (release date March 10, 2013; 247 209 sequences); taxonomy=Viridiplantae; peptide mass tolerance of ±0.3 Da; fragment mass tolerance of ±0.3 for CID ions, in agreement with our recent publications;[50] enzyme specificity trypsin with two missed cleavages considered; fixed modifications: carbamidomethyl (C); variable modifications: oxidation (M).

Metabolomics. Leaves (200 mg per group, four biological replicates per group − the same plants from which samples for proteomics analyses were collected) were finely ground in liquid nitrogen, and powder was used for metabolomics extractions and subsequent analyses. Extraction and metabolomics analyses were performed as previously reported.[51] In brief, powder was collected in separated tubes, and a volume of 0.15 mL of ice cold ultrapure water (18 mΩ) was added. Tubes were then plunged into a water bath at 37 °C for 0.5 min. Samples were mixed with 0.6 mL of −20 °C methanol and then with 0.45 mL of chloroform. Subsequently, 0.15 mL of ice-cold ultrapure water was added to each tube, and they were transferred to a −20 °C freezer for 2−8 h. An equivalent volume of acetonitrile was added to the tube and transferred to a refrigerator (4 °C) for 20 min. Samples with precipitated proteins were thus centrifuged at 10 000g for 10 min at 4 °C.

Finally, samples were dried in a rotational vacuum concentrator (RVC 2−18 − Christ; Osterode am Harz, Germany) and resuspended in 200 mL of water, 5% formic acid and transferred to glass autosampler vials for LC/MS analysis.

HPLC and MS settings were configured as previously reported.[52]

Rapid Resolution Reversed-Phase HPLC. An Ultimate 3000 Rapid Resolution HPLC system (LC Packings, DIONEX, Sunnyvale, USA) was used to perform metabolite separation. The system featured a binary pump and a vacuum degasser, a well-plate autosampler with a six-port microswitching valve, and a thermostatted column compartment. Samples were loaded onto a Reprosil C18 column (2.0 mm × 150 mm, 2.5 mm − Dr. Maisch) for metabolite separation.

Chromatographic separations were achieved at a column temperature of 30 °C and a flow rate of 0.2 mL/min.

For downstream positive ion mode (+) MS analyses, a 0−100% linear gradient of solvent A (ddH2O, 0.1% formic acid) to B (acetonitrile, 0.1% formic acid) was employed over 30 min, returning to 100% A in 2 min and a 6 min post-time solvent A hold.

Mass Spectrometry: Q-TOF Settings. Mass spectrometry analysis was carried out on an electrospray hybrid quadrupole time-of flight mass spectrometer MicroTOF-Q (Bruker-Daltonik, Bremen, Germany) equipped with an ESI ion source. Mass spectra for metabolite extracted samples were acquired both in positive and in negative ion mode. ESI capillary voltage was set at 4500 V (+) ion mode. The liquid nebulizer was set to 27 psi and the nitrogen drying gas was set to a flow rate of 6 L/min. The dry gas temperature was maintained at 200 °C. Data were acquired with a stored mass range of m/z 50−1200. Automatic isolation and fragmentation (AutoMSn mode) was performed on the four most intense ions simultaneously throughout the whole scanning period (30 min per run) to validate metabolite identifications, although peak area quantifications were performed on intact mass spectra, as previously reported.[52]

Instrument calibration was performed externally every day with a sodium formate solution consisting of 10 mM sodium hydroxide in 50% isopropanol: water, 0.1% formic acid. Automated internal mass scale calibration was performed through direct automated injection of the calibration solution at the beginning and at the end of each run by a six-port divert-valve.

Data Elaboration and Statistical Analysis. To reduce the number of possible hits in molecular formula generation, we exploited the SmartFormula3D software (Bruker Daltonics, Bremen, Germany), which directly calculates molecular formulas based on the MS spectrum (isotopic patterns) and transition fingerprints (fragmentation patterns). This software generates a confidence-based list of chemical formulas on the basis of the precursor ions and all fragment ions and the significance of their deviations to the predicted intact mass and fragmentation pattern. Triplicate runs for each one of the four biological replicates were exported as mzXML files and processed through MAVEN.[53] Mass spectrometry chromatograms were elaborated for peak alignment, matching and comparison of parent and fragment ions, and tentative metabolite identification (within a 20 ppm mass-deviation range between observed and expected results against the imported KEGG database[54]). MAVEN is an open-source software that can be freely downloaded from the official project web site (http://genomics-pubs.princeton.edu/mzroll/index.php?show=download). Metabolite assignment was further elaborated in the light of the hydrophobicity/hydrophilicity of the compound and its relative retention time in the RP-HPLC run (as gleaned through database information and preliminary calibration with commercially available ultrapure standards, as previously described). Relative quantitative variations of intact

mass peak areas for each metabolite assigned through MS were normalized against controls (0 μM $CdCl_2$) and plotted with GraphPad Prism 5.0 (GraphPad Software).

Pigment Determination by HPLC. Pigments were extracted from samples by grinding the leaves in liquid nitrogen with degassed 100% acetone at 0−4 °C as previously reported[14] using RP-HPLC equipped with diode array detector for unambiguous identification of each xantophyll. The method was calibrated by injecting known amounts of pure pigments and plotting the peak area (integrator counts) versus quantity of pigment injected.

3. RESULTS AND DISCUSSIONS

First of all, it is worthwhile to note that most of the physiological parameters assayed in the present study (hereby reported as Supporting Information) had been already monitored in previous reports in the literature, as detailed below. However, we decided to repeat these assays to make sure that the system was responding as expected and, more importantly, to allow us to examine the entirety of the response at the proteome/metabolome/physiology levels in the same tissues so that we could have a broader and multitiered view of the Cd effects on *B. juncea*.

Physiological Data

Cd Accumulation Resulted in Reduced Plant Growth, Accumulation in Roots and Shoots, and Altered Ion Homeostasis. Exposure of *B. juncea* to $CdCl_2$ is known to negatively affect plant growth rate to a significant extent.[13] In agreement with the literature, in the present study the overall plant growth (Supplementary Figure 1 in the Supporting Information) and dry weight of shoots and roots (Supplementary Figure 2 in the Supporting Information) were inversely proportional to the concentration of $CdCl_2$ the plants had to cope with.

Although the mechanisms involved in Cd mobility in *Brassicaceae* have been largely documented,[29,30,34,37,40] we hereby determined via ICP MS Cd accumulation in shoots and roots of *B. juncea* (Supplementary Figure 3 in the Supporting Information). As a result, we could observe that Cd accumulation in the roots was proportional to the concentration of $CdCl_2$ (up to ≈11.85 mg of Cd per g dry weight in the roots − Supplementary Figure 3 in the Supporting Information). On the other hand, the diagram representing Cd transport to the shoots followed a Michaelis−Menten-like curve, whereby plant exposure to 25 μM of $CdCl_2$ resulted in approximately 0.4 mg of Cd per g of dry weight, while at 100 μM of $CdCl_2$, Cd concentration in the shoots only increased up to 550 μg per g of dry weight (Supplementary Figure 3 in the Supporting Information). This is suggestive that, above a certain threshold (25 μM of $CdCl_2$), *B. juncea* copes with Cd stress by tuning down its uptake from the soil. This is consistent with previous observations, whereby this phenomenon was justified by a massive coordination of Cd atoms via phytochelatins in the roots.[40]

Cd uptake in the Indian mustard *B. juncea* is known to influence ion homeostasis.[29,30,35,40] In particular, plants exposed to Cd have been previously shown to accumulate potassium (K^+) in the roots[35] and suffer from altered calcium (Ca^{2+}) uptake, which, however, does not significantly affect the homeostasis of other divalent ions (such as Mg^{2+})[40] (Supplementary Figure 4 in the Supporting Information). Indeed, Cd is a Ca^{2+} channel blocker (in that Cd competes with Ca^{2+} for its internalization),[55−59] and Cd interferes with the Ca^{2+} messenger system by binding calmodulin, a Ca^{2+}-binding protein that regulates a variety of enzymes and cell processes.[60] Therefore, alterations of Ca^{2+} homeostasis also result in the deregulation of Ca^{2+}-mediated signaling, with pleiotropic consequences for the plant.[55] Hereby we provide confirmatory evidence about potassium accumulation in the roots and Ca^{2+} internalization increasing in the roots, especially at low-intermediate $CdCl_2$ concentrations (up to 50 μM − Supplementary Figure 4.A in the Supporting Information). This is relevant in that calcium is known to alleviate Cd toxicity by strengthening the photosynthetic system in other *Brassicaceae*.[55] Nitrogen (N) concentration in roots and shoots was not evidently altered by the presence of Cd (Supplementary Figure 4.D in the Supporting Information).

Prolonged Exposure to Cd Resulted in Impaired Transpiration and Water Use Efficiency. Cd stress is known to depress seedling growth through the reduction of stomatal conductance (Gs) and transpiration rate (Tr).[55] It has been shown that abscisic acid can alleviate Cd stress in *B. juncea* by causing a large increase in the stomatal diffusive resistance of leaves, which results in a dramatic reduction in the accumulation of Cd in the leaves.[40] On the basis of this evidence, it has been posited that Cd accumulation in leaves is driven mainly by mass flow due to transpiration.[40] These results were confirmed in the present study as well (Supplementary Table 1 in the Supporting Information), as we observed a decrease in the transpiration rate values and stomatal conductance (halved at 50 and 100 μM $CdCl_2$ concentrations) accompanied by only moderate additional accumulation of Cd in the shoots (Supplementary Figure 2 in the Supporting Information). Besides, we could observe a decrease in the variation of Pn (net CO_2 assimilation - 1/3 in plants exposed to 50 and 100 μM $CdCl_2$ in comparison with controls), while intercellular CO_2 increased significantly ($p < 0.05$ ANOVA) already at 25 μM $CdCl_2$ concentrations (Supplementary Table 1 in the Supporting Information), consistent with the literature.[55,61]

Analogously, water use efficiency decreased significantly upon Cd treatment ($p < 0.05$ ANOVA), and the effects were already evident in 25 μM $CdCl_2$ samples, in agreement with Vrettos et al.[62]

Cd Promoted Pigment Deregulation and Chlorosis Thus Impairing Photosystem II Activity. One of the most evident effects induced by Cd toxicity is leaf chlorosis[8] (Supplementary Figure 1 in the Supporting Information), a phenomenon that is mainly triggered by preferential loss of chlorophylls, especially of chlorophyll *b*.[63] Consistent with the literature, we could observe a significant decrease in the levels of chlorophylls (Supplementary Figure 5 in the Supporting Information), especially in the 25 and 50 μM $CdCl_2$ samples. Minor decreases were observed in the levels of carotene (Supplementary Figure 5, Supplementary Table 2 in the Supporting Information). With respect to the other pigments, only lutein concentration decreased proportionally to Cd concentration (Supplementary Table 2 in the Supporting Information − reporting diode array fast HPLC spectra and the relative light absorbance values for each pigment), while the other pigments (neoxanthin, violoaxanthin, anteroxanthin, zeaxanthin) showed no evident deviations from untreated controls.

In the light of the alterations targeting chlorophylls and lutein, exposure to Cd resulted in the impairment of the

dx.doi.org/10.1021/pr400793e | J. Proteome Res. XXXX, XXX, XXX−XXX

Table 1. Proteomics Responses to Cadmium Exposure in *Brassica juncea*

25 μM vs control							
spot no.	protein ID	Mr, Da theor	pI theor	NCBI GI no.	no. of peptides (high confidence assignments (>95%))	Mascot score	TREND 25 μM Cd vs control
1211	chlorophyll *a/b* binding protein *[Pisum sativum]*	28767	5.24	gil20671	2	85	−1.78
2306	chlorophyll *a/b* binding protein *[Brassica oleracea]*	29142	5.96	gil31323256	5	321	−1.82
2307	chloroplast photosystem II light-harvesting complex protein type III, partial *[Oxytropis maydelliana]*	19748	4.99	gil359754919	5	252	−2.17
2309	chlorophyll *a/b* binding protein 1, chloroplastic; AltName: Full=LHCII type I CAB-1; Short=LHCP; Flags: Precursor	28328	5.17	gil115778	5	291	−1.79
2313	chlorophyll *a/b* binding protein *[Brassica oleracea]*	29142	5.96	gil31323256	4	187	−2.22
2315	ATP synthase CF1 alpha subunit *[Arabidopsis thaliana]*	55351	5.19	gil7525018	2	83	−3.45
	putative nuclear envelope protein lamin intermediate filament superfamily *[Desmodus rotundus]*	52463	5.00	gil417401704	9	495	
2505	HCF136 *[Arabidopsis lyrata subsp. lyrata]*	42991	7.71	gil297808307	13	625	−2.04
	sedoheptulose-1,7-bisphosphatase, chloroplastic	42547	6.04	gil1173347	2	92	
	phosphoribulokinase	44486	6.03	gil125578	5	226	
2706	AtpB gene product (chloroplast) *[Brassica napus]*	53771	5.14	gil383930460	17	886	−1.82
3201	ATP synthase subunit beta, chloroplastic	53740	5.21	gil75336517	4	302	−2.38
3705	AtpA gene product (chloroplast) *[Brassica napus]*	55325	5.14	gil383930459	26	1246	−1.72
	AtpB gene product (chloroplast) *[Brassica napus]*	53771	5.14	gil383930460	18	962	
3806	AtpB gene product (chloroplast) *[Brassica napus]*	53771	5.14	gil383930460	21	1085	−8.33
3813	AtpB gene product (chloroplast) *[Brassica napus]*	53771	5.14	gil383930460	20	1143	−3.85
4205	oxygen-evolving enhancer protein 2, chloroplastic	28079	6.84	gil131391	2	97	−2.27
4302	chloroplast photosystem II light-harvesting complex protein type III, partial *[Oxytropis maydelliana]*	19748	4.99	gil359754919	8	380	−1.78
4701	AtpA gene product (chloroplast) *[Brassica napus]*	55325	5.14	gil383930459	18	768	−1.82
5204	light-harvesting complex I chlorophyll *a/b* binding protein Lhca1	26222	6.22	gil312282193	5	241	−3.70
5302	proteasome subunit beta type-6 *[Arabidopsis thaliana]*	25193	5.31	gil15235889	7	418	−1.85
	PSI type III chlorophyll *a/b*-binding protein *[Arabidopsis thaliana]*	29085	8.61	gil430947	5	321	
5502	AT4g38970/F19H22_70 *[Arabidopsis thaliana]*	43029	6.79	gil16226653	14	599	−3.03
	ATP synthase gamma chain, chloroplast precursor *[Arabidopsis thaliana]*	33475	6.12	gil5708095	5	215	
	enoyl-[acyl-carrier protein] reductase *[Brassica napus]*	40944	9.30	gil14422255	5	160	
	oxidoreductase *[Arabidopsis lyrata subsp. lyrata]*	40983	7.62	gil297850846	3	99	
6203	putative delta subunit of ATP synthase *[Brassica rapa]*	14862	9.19	gil1480014	15	744	−2.04
6204	ribulose-1,5-bisphosphate carboxylase/oxygenase large subunit *[Brassica juncea]*	26358	6.39	gil290586314	5	188	−2.78
6401	ferredoxin-NADP+ reductase *[Arabidopsis lyrata subsp. lyrata]*	40828	8.65	gil297794397	3	90	−1.85
	hypothetical protein ARALYDRAFT_494462 *[Arabidopsis lyrata subsp. lyrata]*	41097	6.85	gil297791273	2	83	
6508	not identified						−2.27
7203	RuBisCO ssu precursor *[Brassica napus]*	20529	7.63	gil17855	8	347	−7.14
	superoxide dismutase *[Raphanus sativus]*	23791	5.96	gil3114705	7	325	
	chloroplast beta-carbonic anhydrase *[Brassica napus]*	36127	5.47	gil297787439	8	322	
0306	RNA-binding protein cp31 *[Arabidopsis lyrata subsp. lyrata]*	33599	4.89	gil297799522	20	422	+2.73
	ribulose bisphosphate carboxylase large chain; Short=RuBisCO large subunit	52030	6.00	gil17367562	7	165	
	hypothetical protein ARALYDRAFT_918033 *[Arabidopsis lyrata subsp. lyrata]*	32140	4.93	gil297795791	7	161	
	glycine-rich RNA-binding protein 5 *[Arabidopsis thaliana]*	28768	4.61	gil15221187	5	130	
0406	plastid-lipid associated protein PAP2 *[Brassica rapa subsp. campestris]*	34689	4.79	gil14248550	25	508	+2.30

dx.doi.org/10.1021/pr400793e | J. Proteome Res. XXXX, XXX, XXX−XXX

Table 1. continued

25 μM vs control							
spot no.	protein ID	Mr, Da theor	p*I* theor	NCBI GI no.	no. of peptides (high confidence assignments (>95%))	Mascot score	TREND 25 μM Cd vs control
	similar to nascent polypeptide associated complex alpha chain *[Arabidopsis thaliana]*	25580	4.21	gil4115918	12	219	
	molecular chaperone GrpE *[Arabidopsis thaliana]*	35529	4.57	gil18418410	8	208	
	RNA-binding protein cp33 *[Arabidopsis lyrata subsp. lyrata]*	36301	4.67	gil297816516	11	202	
0505	plastid-lipid associated protein PAP3 *[Brassica rapa subsp. campestris]*	39278	4.55	gil14248552	6	129	+3.48
0811	putative chlorophyll *a*/*b* binding protein *[Phalenopsys hybrid]*	29702	5.48	gil4512125	3	76	+34.13
1206	2-cys peroxiredoxin, chloroplast *[Arabidopsis lyrata subsp. lyrata]*	29143	6.11	gil297829716	22	444	+1.55
	soul heme-binding family protein *[Arabidopsis lyrata subsp. lyrata]*	25668	4.69	gil297844644	4	83	
1417	hypothetical protein ARALYDRAFT_914391 *[Arabidopsis lyrata subsp. lyrata]*	33899	8.62	gil297799794	10	236	+2.93
	putative plastid-lipid-associated protein 1 *[Arabidopsis thaliana]*	34984	5.45	gil15233357	6	158	
1708	ribulose bisphosphate carboxylase large chain; Short=RuBisCO large subunit	53436	5.88	gil1346967	85	991	+4.48
1812	ribulose-1,5-bisphosphate carboxylase/oxygenase large subunit *[Phyllacanthus grisebachianus]*	46990	6.56	gil298568046	5	110	+10.28
2314	143−3 (14−3−3 protein) *[Brassica napus]*	29002	4.79	gil224981577	32	489	+1.99
	GF14 omega *[Brassica napus]*	29223	4.68	gil13447104	22	418	
	hypothetical protein ARALYDRAFT_494127 *[Arabidopsis lyrata subsp. lyrata]*	28989	4.73	gil297805908	14	265	
2407	plastid-lipid associated protein PAP1 *[Brassica rapa subsp. campestris]*	35714	5.32	gil14248548	5	180	+2.08
	fibrillin *[Brassica napus]*	25858	5.12	gil4139097	4	170	
4301	chloroplast beta-carbonic anhydrase *[Brassica napus]*	36127	5.47	gil297787439	23	410	+2.89
	predicted protein *[Arabidopsis lyrata subsp. lyrata]*	27425	5.39	gil297816838	17	377	
	chaperonin 10 *[Arabidopsis thaliana]*	26912	8.86	gil3057150	25	327	
	triosephosphate isomerase *[Arabidopsis thaliana]*	33553	7.67	gil15226479	7	133	
	putative plastid-lipid-associated protein 6 *[Arabidopsis thaliana]*	30493	5.82	gil18403751	5	121	
4403	thiazole biosynthetic enzyme *[Arabidopsis thaliana]*	36755	5.82	gil15239735	7	113	+1.92
5508	fructose-bisphosphate aldolase, class I *[Arabidopsis thaliana]*	43132	6.79	gil18420348	13	621	+3.81
	cysteine synthase *[Arabidopsis thaliana]*	41976	8.13	gil572517	2	96	

100 μM vs Control				
spot no.	protein ID	Mr, Da theor	p*I* theor	NCBI GI no.
1409	33 kDa oxygen-evolving protein *[Arabidopsis thaliana]*	35285	5.68	gil22571
	Inorganic pyrophosphatase family protein *[Arabidopsis lyrata subsp. lyrata]*	33693	6.03	gil297811059
	N-glyceraldehyde-2-phosphotransferase-like *[Arabidopsis thaliana]*	31998	5.14	gil8885622
2402	oxygen-evolving enhancer protein 1−2 *[Arabidopsis thaliana]*	35226	5.92	gil15230324
2505	HCF136 *[Arabidopsis lyrata subsp. lyrata]*	42991	7.71	gil297808307
	sedoheptulose-1,7-bisphosphatase, chloroplastic	42547	6.04	gil1173347
	phosphoribulokinase	44486	6.03	gil125578
2603	putative delta subunit of ATP synthase *[Brassica rapa]*	14862	9.19	gil1480014
3201	ATP synthase subunit beta, chloroplastic	53740	5.21	gil75336517
3806	AtpB gene product (chloroplast) *[Brassica napus]*	53771	5.14	gil383930460
3812	AtpB gene product (chloroplast) *[Brassica napus]*	53771	5.14	gil383930460
	chloroplast ribulose-1,5-bisphosphate carboxylase/oxygenase activase *[Brassica oleracea]*	48086	6.78	gil383470439
3813	AtpB gene product (chloroplast) *[Brassica napus]*	53771	5.14	gil383930460
4506	hypothetical protein ARALYDRAFT_482998 *[Arabidopsis lyrata subsp. lyrata]*	52208	5.69	gil297827581
5204	light-harvesting complex I, chlorophyll *a*/*b* binding protein Lhca1	26222	6.22	gil312282193
5405	ferredoxin-NADP+ reductase *[Arabidopsis lyrata subsp. lyrata]*	40828	8.65	gil297794397
5506	AT4g38970/F19H22_70 *[Arabidopsis thaliana]*	43029	6.79	gil16226653
6204	ribulose-1,5-bisphosphate carboxylase/oxygenase large subunit *[Brassica juncea]*	26358	6.39	gil290586314
6205	superoxide dismutase *[Raphanus sativus]*	23791	5.96	gil3114705

dx.doi.org/10.1021/pr400793e | *J. Proteome Res.* XXXX, XXX, XXX−XXX

Table 1. continued

100 μM vs Control				
spot no.	protein ID	Mr, Da theor	p*I* theor	NCBI GI no.
	RuBisCO ssu precursor *[Brassica napus]*	20529	7.63	gil17855
6401	ferredoxin-NADP+ reductase *[Arabidopsis lyrata subsp. lyrata]*	40828	8.65	gil297794397
	hypothetical protein ARALYDRAFT_494462 *[Arabidopsis lyrata subsp. lyrata]*	41097	6.85	gil297791273
7202	ribulose-1,5-bisphosphate carboxylase/oxygenase small subunit precursor *[Brassica rapa]*	20541	8.23	gil119720784
0505	plastid-lipid associated protein PAP3 *[Brassica rapa subsp. campestris]*	39278	4.55	gil14248552
1416	Plastid-lipid associated protein PAP1 *[Brassica rapa subsp. campestris]*	35714	5.32	gil14248548
1417	hypothetical protein ARALYDRAFT_914391 *[Arabidopsis lyrata subsp. lyrata]*	33899	8.62	gil297799794
	putative plastid-lipid-associated protein 1 *[Arabidopsis thaliana]*	34984	5.45	gil15233357
	plastid lipid-associated protein 1, chloroplast precursor *[Arabidopsis lyrata subsp. lyrata]*	35224	5.35	gil297809587
1708	ribulose bisphosphate carboxylase large chain; Short=RuBisCO large subunit	53436	5.88	gil1346967
2605	glutamine synthetase *[Brassica napus]*	47889	6.37	gil6966930
2702	ATP synthase CF1 beta subunit *[Brassica napus]*	53771	5.14	gil262400757
	RuBisCO large subunit partial *[Brassica napus]*	50643	5.95	gil340510942
	ATP synthase beta subunit *[Brassica balearica]*	51343	5.12	gil14717970
3302	chlorophyll *a*/*b* binding protein *[Brassica oleracea]*	29142	5.96	gil31323256
	cytosolic triose phosphate isomerase *[Arabidopsis thaliana]*	27366	5.24	gil414550
3610	unnamed protein product *[Thellungiella halophila]*	48202	6.08	gil312281705
	hypothetical protein ARALYDRAFT_482998 *[Arabidopsis lyrata subsp. lyrata]*	52208	5.69	gil297827581
	ribulose bisphosphate carboxylase/oxygenase activase *[Arabidopsis thaliana]*	52347	5.87	gil18405145
	adenosine kinase 1 *[Arabidopsis thaliana]*	38268	5.29	gil15232763
5508	fructose-bisphosphate aldolase, class I *[Arabidopsis thaliana]*	43132	6.79	gil18420348
	cysteine synthase *[Arabidopsis thaliana]*	41976	8.13	gil572517

100 μM vs 25 μM							
spot no.	protein ID	Mr, Da Theor	p*I* Theor	NCBI GI No.	no. of peptides (high confidence assignments (>95%))	Mascot score	TREND 100 μM Cd vs 25 μM
0306	RNA-binding protein cp31 *[Arabidopsis lyrata subsp. lyrata]*	33599	4.89	gil297799522	20	422	**−3.03**
	ribulose bisphosphate carboxylase large chain; Short=RuBisCO large subunit	52030	6.00	gil17367562	7	165	
	hypothetical protein ARALYDRAFT_918033 *[Arabidopsis lyrata subsp. lyrata]*	32140	4.93	gil297795791	7	161	
	glycine-rich RNA-binding protein 5 *[Arabidopsis thaliana]*	28768	4.61	gil15221187	5	130	
1105	ribosomal protein L12 *[Arabidopsis thaliana]*	66197	8.15	gil468773	2	132	−1.72
1601	small subunit ribosomal protein S1 *[Arabidopsis thaliana]*	45310	5.13	gil30692346	8	441	−2.04
1602	small subunit ribosomal protein S1 *[Arabidopsis thaliana]*	45310	5.13	gil30692346	6	293	−1.72
1701	RuBisCO large subunit-binding protein subunit alpha, chloroplastic	61682	5.14	gil464727	17	977	−1.72
2601	chloroplast ribulose-1,5-bisphosphatee carboxylase/oxygenase activase *[Brassica oleracea]*	48086	6.78	gil383470439	4	146	−2.86
2603	putative delta subunit of ATP synthase *[Brassica rapa]*	14862	9.19	gil1480014	2	124	−1.89
2606	small subunit ribosomal protein S1 *[Arabidopsis thaliana]*	45310	5.13	gil30692346	14	631	−1.59
2711	heat shock protein 70 *[Arabidopsis thaliana]*	77230	5.13	gil6746592	12	507	−2.94
2717	RuBisCO large subunit-binding protein subunit alpha, chloroplastic	61682	5.14	gil464727	21	1197	−2.08
4301	chloroplast beta-carbonic anhydrase *[Brassica napus]*	36127	5.47	gil297787439	23	410	−1.67
	predicted protein *[Arabidopsis lyrata subsp. lyrata]*	27425	5.39	gil297816838	17	377	
	chaperonin 10 *[Arabidopsis thaliana]*	26912	8.86	gil3057150	25	327	
	triosephosphate isomerase *[Arabidopsis thaliana]*	33553	7.67	gil15226479	7	133	
	putative plastid-lipid-associated protein 6 *[Arabidopsis thaliana]*	30493	5.82	gil18403751	5	121	
1211	chlorophyll *a*/*b*-binding protein *[Pisum sativum]*	28767	5.24	gil20671	2	85	+1.71

dx.doi.org/10.1021/pr400793e | *J. Proteome Res.* XXXX, XXX, XXX−XXX

Table 1. continued

100 μM vs 25 μM							
spot no.	protein ID	Mr, Da Theor	p*I* Theor	NCBI GI No.	no. of peptides (high confidence assignments (>95%))	Mascot score	TREND 100 μM Cd vs 25 μM
2306	chlorophyll *a*/*b* binding protein *[Brassica oleracea]*	29142	5.96	gil31323256	5	321	+2.68
2309	chlorophyll *a*/*b* binding protein 1, chloroplastic; AltName: Full=LHCII type I CAB-1; Short=LHCP; Flags: Precursor	28328	5.17	gil115778	5	291	+1.71
2313	chlorophyll *a*/*b* binding protein *[Brassica oleracea]*	29142	5.96	gil31323256	4	187	+1.73
2315	ATP synthase CF1 alpha subunit *[Arabidopsis thaliana]*	55351	5.19	gil7525018	2	83	**+3.38**
	putative nuclear envelope protein lamin intermediate filament superfamily *[Desmodus rotundus]*	52463	5.00	gil417401704	9	495	
3201	ATP synthase subunit beta, chloroplastic	53740	5.21	gil75336517	4	302	+1.57

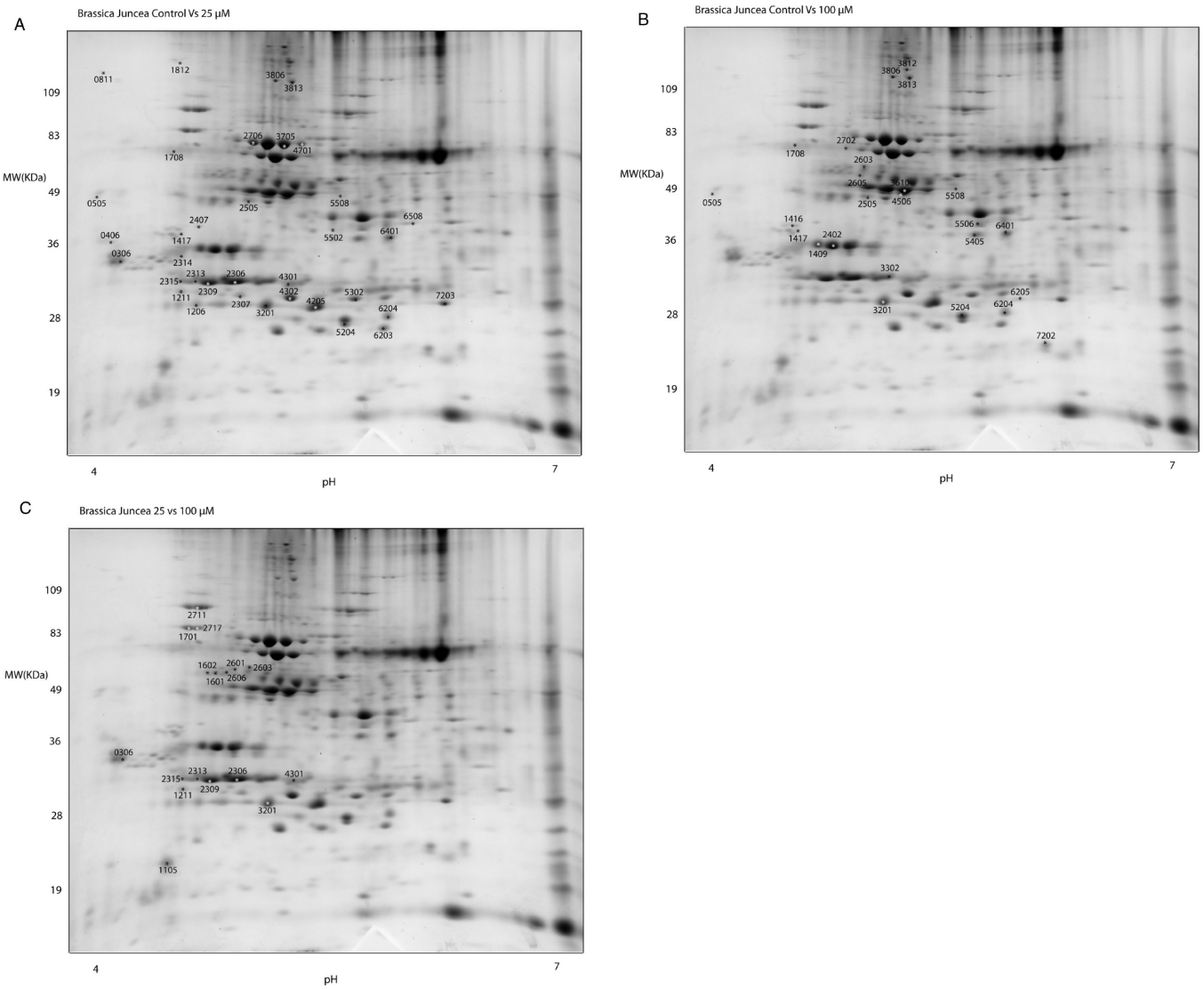

Figure 1. Representative gel from 2DE analysis of *B. juncea* leaves exposed to 25 or 100 μM $CdCl_2$ in comparison with untreated controls. Statistically significant differential spots (p value < 0.05 and fold change >1.5) for control versus 25 μM analyses are reported in panel A, while in panel B we indicated those spots showing statistically significant variations in controls in comparison with leaves exposed to 100 μM $CdCl_2$. Panel C shows spots differing between 25 and 100 μM gels. Spot protein identifications are reported in Table 1. Molecular weight (MW) and p*I* range of the first dimension strips (4−7) are indicated on the appropriate axis.

dx.doi.org/10.1021/pr400793e | *J. Proteome Res.* XXXX, XXX, XXX−XXX

photosystem II (PSII) activity, especially at high $CdCl_2$ concentrations (50−100 μM - Supplementary Table 3 in the Supporting Information). Indeed, the prolonged exposure to Cd (21 days in the present study) allows us to appreciate such changes, which remained hitherto undisclosed in previous studies assaying the effects of Cd treatment during a shorter time-span (96 h in Haag-Karwer et al.[61]). In detail, the maximum quantum yield of PSII (calculated as F_v/F_m), and the effective quantum efficiency of PSII moderately decreased upon exposure to 25 μM $CdCl_2$, consistent with Haag-Kerwer et al.[61] (25 μM $CdNO_3$), although the drop in F_v/F_m and Q_{PSII} values was more evident at higher doses (50−100 μM) of $CdCl_2$ (Supplementary Table 3 in the Supporting Information − Taamalli et al, in preparation). The partial values for F_o (minimum fluorescence level in the dark-adapted state), F_m (maximum fluorescence level in the dark-adapted state), and F_v (variable fluorescence) decreased significantly in 25 μM samples (Supplementary Table 3 in the Supporting Information). Notably, 50 and 100 μM Cd concentrations resulted in more evident reductions of quantum yield of PSII (Supplementary Table 3 in the Supporting Information), suggesting that intermediate Cd concentrations might be tolerated by the plant with only partially detrimental effects in terms of potential photosystem efficiency.

From Physiology to Proteomics and Metabolomics. *B. juncea* (accession 426308) accumulated Cd in the shoots at concentration largely exceeding the threshold of qualification of hyperaccumulator species (100 ppm), which is an argument supporting the classification of this species as a Cd-hyperaccumulator. High Cd accumulation was accompanied by a reduced accumulation of biomass (reaching 30% in plants subjected to Cd in comparison with control ones). This growth retardation could be the result of the disturbances of physiological processes such nutrient acquisition and translocation, photosynthetic pigment biosynthesis inhibition-induced chlorosis, and thus the impairment of photosystem II activity. Cd in the nutrient solution could be also responsible for the restriction of water absorption, leading to the dehydration of and subsequently to stomata closure and the inhibition of the entry of CO_2. Despite physiological disturbances and growth retardation, preservation of biomass production under acute Cd stress (100 μM) suggests that tolerance and accumulation of Cd in this species is utterly governed by several proteomic and metabolic mechanisms.

Proteomics

Because Cd stress is known to influence gene expression,[64−66] other than the ultrastructural organization and integrity of proteins and protein complexes,[13] gel-based analyses were performed to assay the responses of the leaf proteome to Cd toxicity. Proteomics approaches to *B. juncea* responses to Cd stress are not novel, although so far leaves were only investigated via native gel analytical strategies[13] or rather papers in the literature were focused on the alterations to the root proteome.[31] Results are detailed in Table 1, whereby spot numbers and their quantitative trends (fold-change variations) in the above-mentioned coupled comparisons are reported, together with the NCBI gene identifier, the theoretical molecular weights and p*I*s, Mascot scores, and the number of peptides identified via nanoHPLC-MS/MS. Further details of protein identifications are provided in the Supplementary File 1 in the Supporting Information, including the raw outputs of Mascot database searches. Raw 2DE gels for each biological replicate for each group (control, 25 and 100 μM $CdCl_2$) are reported in Supplementary Figure 6 in the Supporting Information. Exposure to 25 or 100 μM $CdCl_2$ resulted in the statistically significant (p-value <0.05 ANOVA, fold-change $\geq$ |1.5|) variation in abundance of a total of 58 differential spots across groups (control vs 25 − Figure 1A; control vs 100 − Figure 1B; or 25 vs 100 − Figure 1C).

Differential Proteomics Revealed That Exposure to Mild (25 μM) Cd Stress Resulted in Alteration of the Photosystem, CO_2 Homeostasis, and Energy/Redox Metabolism. In the present study, a comparison of 2DE gels of untreated control leaves against those obtained from the analyses of leaves from plants exposed to 25 μM $CdCl_2$ indicated that Cd treatment resulted in the down-regulation of 23 spots, while 13 spots were up-regulated in response to heavy metal stress (25 μM of $CdCl_2$ − Table 1, Figure 1A). Down-regulated spots include proteins mainly involved in photosynthesis (chlorophyll *a*/*b*-binding proteins and LHC or photosystem II-related proteins − spots no. 1211, 2306, 2309, 2313, 4302, 5204, and 5302; ferredoxin-$NADP^+$ reductase − spot no. 6401 in Table 1). This is not novel in that heavy metal stress is known to promote alterations to the photosystem,[67−72] as confirmed in the present study, in particular, when plants were exposed to higher doses of Cd (Supplementary Table 3 in the Supporting Information).

One of the molecular explanations underlying this phenomenon implies the role of carbonic anhydrase in the stimulation of RuBisCO at low Cd concentrations,[73] a phenomenon that has been largely investigated in Cd hyperacccumulator plants.[74] Furthermore, it is worthwhile recalling that the activity of carbonic anhydrases also relies upon divalent ions (Zn^{2+}) and might thus be affected by Cd. Indeed, carbonic anhydrase is a zinc metalloenzyme catalyzing the reversible hydration of CO_2 to produce H^+ and $HCO3^-$. As described above, in the present study, we could observe alterations in the levels of intercellular carbon dioxide and its net assimilation (Supplementary Table 1 in the Supporting Information). Hereby, prolonged exposure to 25 μM $CdCl_2$ influenced carbon dioxide homeostasis by decreasing the levels of beta carbonic anhydrase (spot no. 7203) and increasing the levels of chloroplast beta-carbonic anhydrase (spot no. 4301) (Table 1, Figure 1A). Differences in the experimental p*I*s of spots no. 7203 and 4301 might be suggestive of a likely post-translational modification event in response to mild Cd stress, in agreement with the literature[75] and by analogy to our previous reports on other biological matrices.[76,77]

Cd-induced down-regulation also involved metabolic enzymes, including proteins involved in energy metabolism (chloroplast ATP synthase subunits − spots nos. 2315, 2706, 3201, 3705, 3806, 3813, 4701, 5502, and 6203 in Table 1, Figure 1A), consistently with our previous native gel-based approaches[13] and Calvin cycle (ribulose-1,5-bisphosphate carboxylase/oxygenase (RuBisCO) − spot nos. 6204, 7203; sedoheptulose 1,7-biphosphatase − spot no. 2505 in Table 1, Figure 1A).

Up-regulated proteins in 25 μM leaves include (i) RNA-binding proteins (spots no. 0306, 0406), previously reported to be up-regulated at the transcriptional level by Cd in *B. juncea*;[65] (ii) plastid lipid associated proteins (spot nos. 0406, 0505, 1417, 2407, and 4301), which are known to accumulate in leaf chloroplasts under abiotic stress conditions and serve either as storage repositories for hydrophobic compounds or in the structural stabilization of thylakoid membranes upon environ-

dx.doi.org/10.1021/pr400793e | J. Proteome Res. XXXX, XXX, XXX−XXX

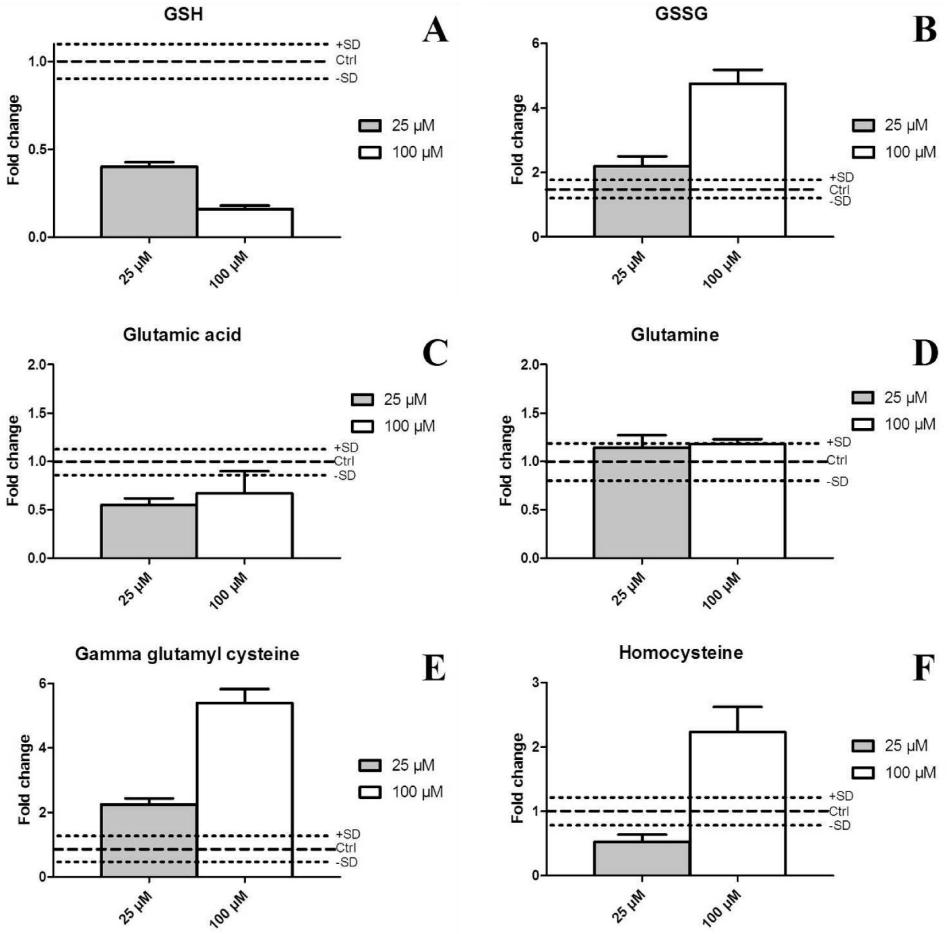

Figure 2. Variation in the levels of metabolites of the glutathione homeostasis (A–F) in the leaves of *Brassica juncea* subjected to different Cd concentration normalized against untreated controls (gaped line at one-fold change, ±SD calculated across normalized biological replicates of control leaves). Measurements were performed in triplicate on pooled ground leaves coming from four individual plants per group (control, 25 and 100 μM).

mental constraints;[78] and (iii) chelating proteins (soul heme-binding family protein – spot no. 1206), oxidative stress proteins (2-cys peroxiredoxin – spot no. 1206), and chaperonin (heats shock proteins (HSPs) – spot no. 4301) or other signaling proteins (143–3 protein of the 14–3–3 protein family – spot no. 2314). As far as HSPs are concerned, their role in plant responses to abiotic stresses is pivotal in mediating ROS-signaling arising upon prolonged Cd exposure.[79] Indeed, Cd-generated ROS act both as oxidative molecules, aggressively reacting with cellular macromolecules, and as signal transduction molecules.[80,81] In terms of phosphorylation signaling (the 143–3 protein is a signaling protein recognizing phophoserine or phosphothreonine motifs), it is interesting to note that MAPK-mediated phosphorylation cascades are known to exert a central role in mediating Cd and heavy metal-stress signaling.[82,83]

Of note, exposure to 25 μM $CdCl_2$ resulted in the up-regulation of metabolic enzymes, including fructose 1-6 biphosphate aldolase (spot no. 5508) and triosephosphate isomerase (spot no. 4301), suggesting either an increased rate in the fluxes from hexose to triose sugars or vice versa (as the enzymes can act in both directions) (Figure 1A and Table 1), a key step in glycolysis or in the promotion of a shift back to the pentose phosphate pathway (PPP) or Calvin cycle. Cd stress also resulted in the up-regulation of cysteine synthase (spot no. 5508) and the thiazole biosynthetic enzyme (spot no. 4403), both involved in sulfur metabolism toward the production of cystein and thiolated purines.

Exposure to Heavy (100 μM) Cd Stress Further Impaired Photosystem Integrity and Metabolic Activity, Especially by Targeting Enzymes Involved in the Calvin Cycle and Glutathione Homeostasis. Electrophoretic analyses of control leaves against those obtained from plants exposed to 100 μM of $CdCl_2$ highlighted the down-regulation of 16 protein spots and the up-regulation of 9. When examining the list of down-regulated proteins (Table 1, Figure 1B), it emerges that the trends observed in the first comparison (controls vs 25 μM – see above) were confirmed (RuBisCO, chloroplast ATP synthase subunits, LHC components, Ferredoxin NADP+ reductase, Sedoheptulose 1,7 biphosphatase – Table 1). Treatment with higher concentrations of Cd also resulted in the peculiar down-regulation of the oxygen evolving enhancer protein 1–2 (spot nos. 1409 and 2402 – Table 1, Figure 1B), a protein involved in the regulation of the dephosphorylation and turnover of the PSII reaction center D1 protein (which in turn is a pivotal component in the core reaction centers and participates in photoinhibition responses).[84]

Up-regulated proteins in 100 μM samples were consistent with the observations in 25 μM leaves, including increased

dx.doi.org/10.1021/pr400793e | J. Proteome Res. XXXX, XXX, XXX–XXX

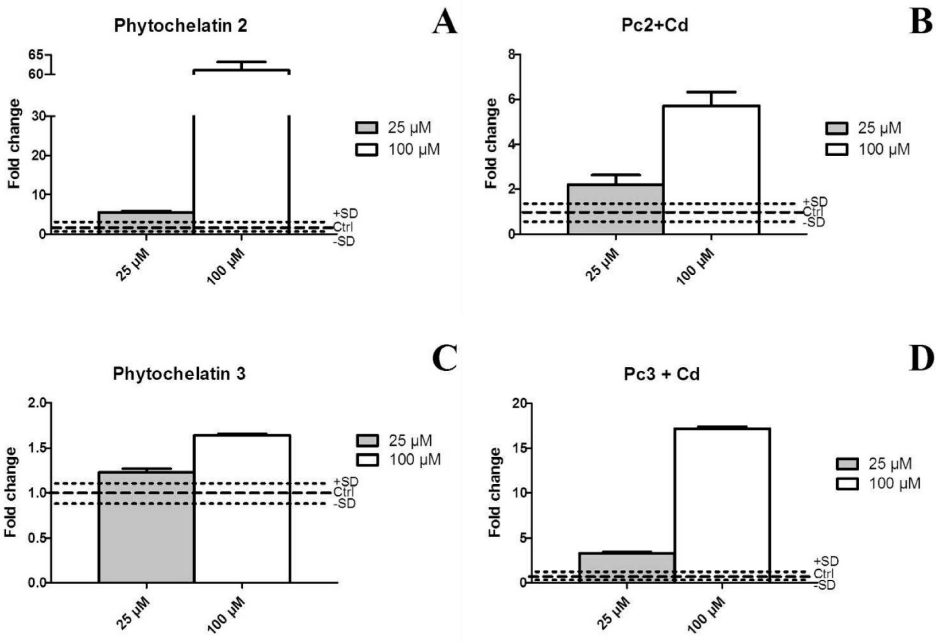

Figure 3. Variation in the levels of metabolites of the phytochelatins and relative cadmium adducts (A–D) in the leaves of *Brassica juncea* subjected to different Cd concentration normalized against untreated controls (gaped line at one-fold change, ±SD calculated across normalized biological replicates of control leaves). Measurements were performed in triplicate on pooled ground leaves coming from four individual plants per group (control, 25 and 100 μM).

photodensities for spots further identified as plastid lipid associated proteins (spots no. 0505, 1416, and 1417), triose phosphate isomerase (no. 3302), and fructose biphosphate aldolase (no. 5508 – Table 1, Figure 1B), in agreement with our previous observations of Cd effect on spinach apical leaves.[14] Higher concentrations of Cd lead to the peculiar increase in the levels of glutamine synthase (spot no. 2605), which might play an indirect role in glutathione homeostasis by fueling glutamate-to-glutamine conversion (glutamate being a rate-limiting substrate for reduced glutathione - GSH biosynthesis) and thus be related to sulfur metabolism (cystein synthase spot no. 5508). This result is consistent with previous findings of up regulation of GS in response to cadmium.[85,86] Glutamine synthetase represents one key enzyme in nitrogen assimilation, which is known to negatively respond in terms of activity to Cd stress in heavy metal sensitive plants.[87] Indeed, glutamine synthase is dependent on divalent ions (Mn^{2+} or Mg^{2+}) to exert its biological activity, and thus Cd might disrupt the biochemistry of the active site. Its up-regulation in the Cd tolerant *B. juncea* might indicate a biological strategy adopted by the plant to cope with a Cd-induced reduction in enzyme activity. Of note, this result is confirmatory of evidence in *B. juncea* at the transcriptional level.[65]

In Comparison with Mild Cd Stress, High Cd Stress Exacerbated Metabolic Effects by Deregulating ATP Synthesis (through the Fragmentation of ATP Synthase Subunits) and by Promoting Membrane Disintegration. A comparison of 2DE gels from 25 and 100 μM leaves was performed to determine protein changes in response to mild and intense Cd stress, respectively (Table 1, Figure 1C). As a result, 11 proteins appeared to be up-regulated during exposure to mild stress, including RNA binding proteins cp31 (spot no. 0306), ribosomal subunits (L12 – no. 1105; S1 – nos. 1601, 1602, 2606), RuBisCO subunits (nos. 0306, 1701, 2717), carbonic anhydrase (no. 4301), and chaperone proteins (no. 2711, 4301).

Heavy metal stress at higher Cd concentrations (100 μM) resulted in the up-regulation of chlorophyll *a*/*b* binding proteins (spots nos. 1211, 2306, 2309, and 2113) and fragmentation of chloroplast ATP synthase subunits because the experimentally observed molecular weights for spot nos. 2315 and 3201 were almost halved in comparison with the theoretically expected ones (Figure 1C, Table 1). This is consistent with our previous observations in Indian mustard, whereby sustained Cd stress results in the fragmentation of the ATP synthase complex.[13] Finally, exacerbation of Cd stress at higher doses resulted in membrane disintegration, as suggested by the presence of a putative fragment of the nuclear envelope protein lamin intermediate filament (spot no. 2315 – Figure 1C and Table 1).

Metabolomics

Metabolomics is rapidly emerging as an innovative tool in the field of research on plant responses to heavy metal stress.[88] Metabolomics analyses were performed on *B. juncea* leaves exposed to 25 or 100 μM $CdCl_2$, and results were compared with those obtained by assaying untreated control leaves. Upon alignment and matching of mass spectra chromatogram and feature detection throughout the whole retention time range, scatter plot analyses including those features present in at least all the replicates of one group in a statistically significant fashion (p-value <0.05 ANOVA) were performed by comparing control runs against 25 and 100 μM Cd counterparts (Supplementary Figures 7 and 8 in the Supporting Information, respectively).

To ease data representation and interpretation, we divided metabolites into the following subgroups by referring to their relative metabolic pathway: (i) glutathione homeostasis (Figure 2), (ii) phytochelatins (Figure 3), (iii) purine metabolism (Supplementary Figure 9 in the Supporting Information); (iv)

dx.doi.org/10.1021/pr400793e | J. Proteome Res. XXXX, XXX, XXX–XXX

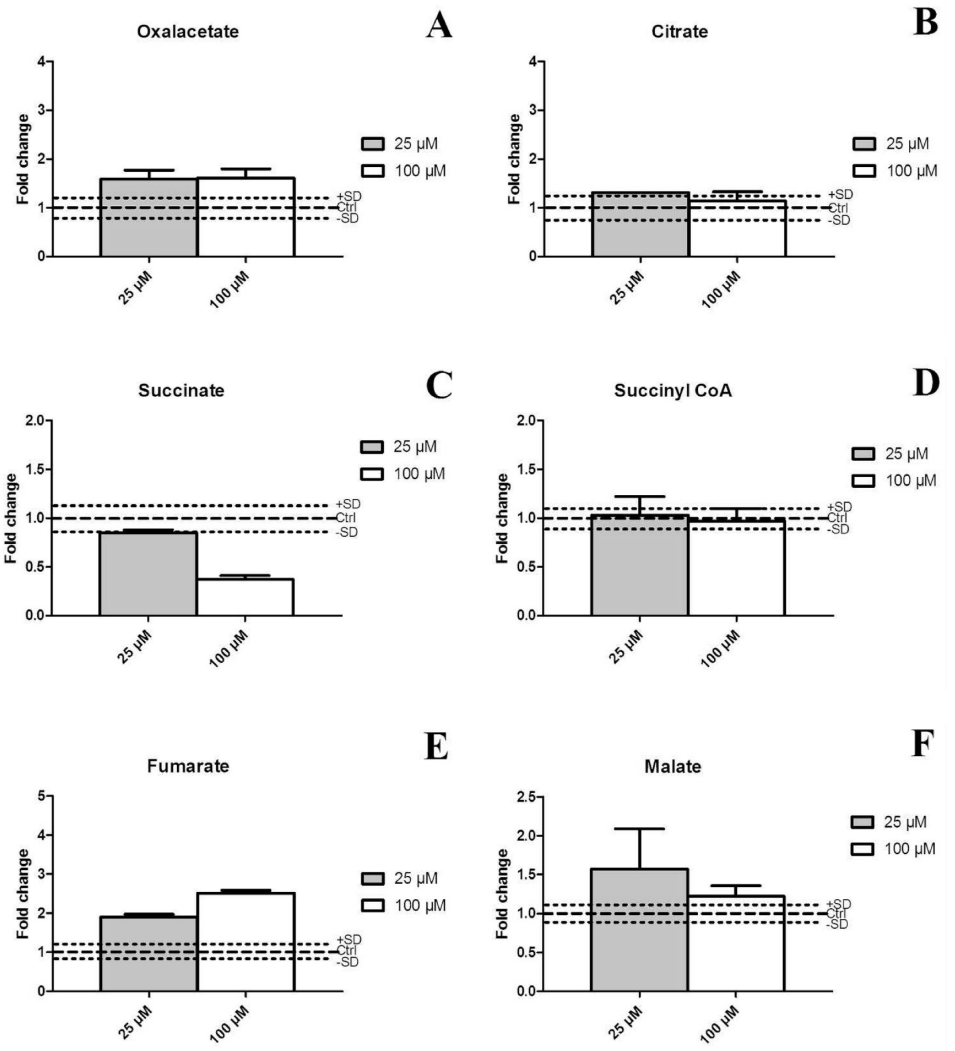

Figure 4. Variation in the levels of metabolites of organic acid of the tricarboxylic acid cycle (A–F) in the leaves of *Brassica juncea* subjected to different Cd concentration normalized against untreated controls (gaped line at one-fold change, ± SD calculated across normalized biological replicates of control leaves). Measurements were performed in triplicate on pooled ground leaves coming from four individual plants per group (control, 25 and 100 μM).

tricarboxylic acid cycle (TCA – Figure 4); (v) glycolysis (Figure 5); (vi) Calvin cycle (Figure 6); and (vii) plant hormones/signaling molecules (Figure 7). Results will be hereby described and integrated with physiological and proteomics data anticipated above, in light of the available literature.

Oxidative Stress: Alterations to Glutathione Homeostasis, Phytochelatins, Sulfur Metabolism, and Cross-Talks with Purine Metabolism. Cd stress is known to promote the generation of ROS, which prompts the accumulation of oxidative stress. In line with the posited hypothesis, GSH decreased (Figure 2A) and GSSG increased (Figure 2B) proportionally to $CdCl_2$ concentration. Alterations to GSH-homeostasis were not attributable to the deregulation of GSH precursor glutamic acid (Figure 2C) and its precursor glutamine (Figure 2D), which did not show major deviation from controls upon Cd exposure. This is consistent with the considerations reported above and borrowed from the literature about the Cd-dependent increase in the transcriptional[65] and protein expression levels (Table 1) of glutamine synthase coping with the Cd-impaired activity of this enzyme, as explained above.

GSH precursors, gamma-glut cysteine (Figure 2E), cysteine (Supplementary Figure 10.A in the Supporting Information), and homocysteine (a precursor to cysteine – Figure 2F) increased proportionally to Cd stress, consistently with the posited up-regulation of sulfur metabolism in response to heavy metal toxicity.[89−94]

GSH homeostasis is also relevant as it represents a sink for the biosynthesis of phytochelatins (PCs). PCs play a pivotal role in detoxification processes, through the direct chelation of heavy metal molecules, which eases their accumulation and transport into vacuoles.[95,96]

By applying a validated MS-based method for the detection of PC and the relative Cd adducts, we could determine that Cd (especially at 100 μM doses), resulted in the significant accumulation of PC2 and PC3 other than of their relative Cd adducts (Figure 3A–D). This is also consistent with recent reports from the literature.[25]

Sulfur metabolism in plants is not only limited to GSH, cysteine and homocysteine. Cross-talks between sulfur and

dx.doi.org/10.1021/pr400793e | J. Proteome Res. XXXX, XXX, XXX–XXX

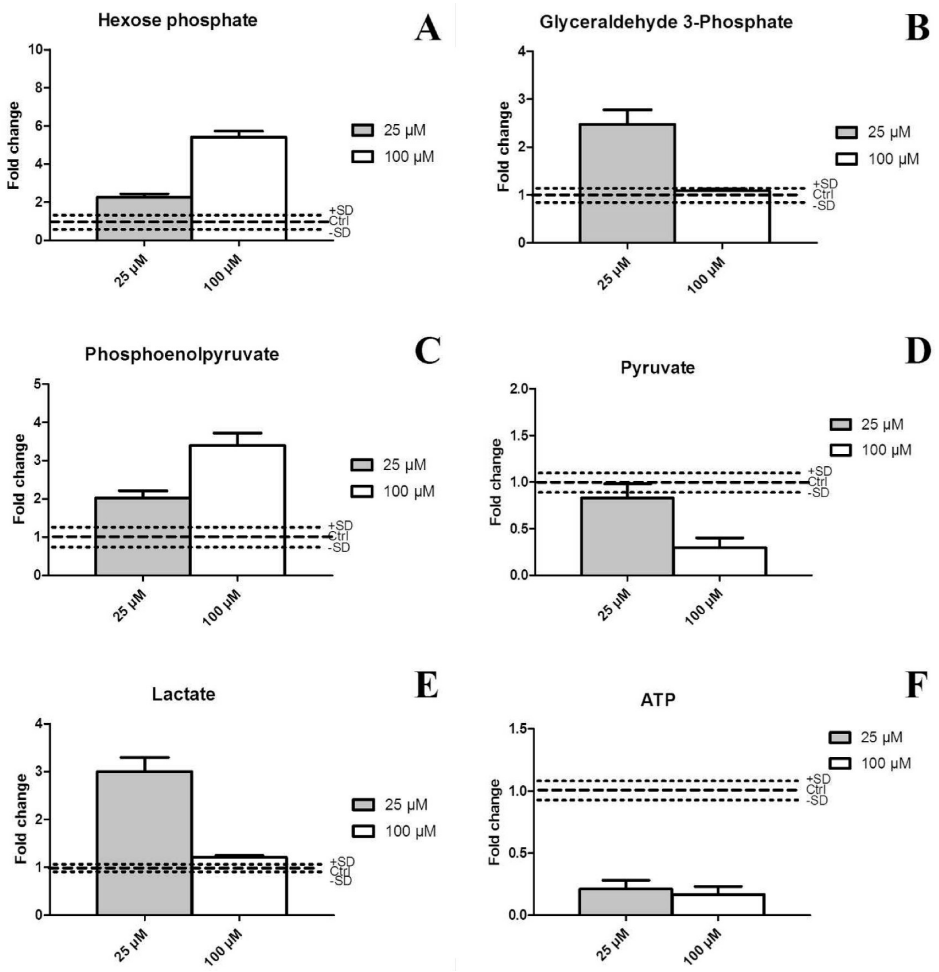

Figure 5. Variation in the levels of metabolites of glycolytic intermediates (A–E) and adenosine triphosphate (ATP) (F) in the leaves of *Brassica juncea* subjected to different Cd concentration normalized against untreated controls (gaped line at one-fold change, ±SD calculated across normalized biological replicates of control leaves). Measurements were performed in triplicate on pooled ground leaves coming from four individual plants per group (control, 25 and 100 μM).

purine metabolism are known to play a role in abiotic stress responses, as they modulate ATP utilization on the one hand and accumulation of thiol-group-containing purines (precursors of thiol-containing metabolites) on the other hand.[97,98]

Genetic analyses of the link between metal complex accumulation and purine biosynthesis enzymes revealed that genetic lesions blocking two segments of the pathway, before and after the IMP branchpoint, are required to produce the Cd-sensitive phytochelatin-deficient phenotype in *Schizosaccaromyces pombe*.[99,100]

In Supplementary Figure 9 in the Supporting Information, we report the trends for a subset of metabolites involved in purine nucleoside metabolism, including adenine (Supplementary Figure 9.A in the Supporting Information), adenosine (B), cyclic AMP (C), AMP (D), ADP (E), sulfur-containing purines adenosyl-homocysteine (F), adenosylhomomethionine (G), hypoxanthine (H), IMP (I), and inosine (J). While hypoxanthine and related nucleoside were not apparently influenced by Cd stress, phosphorylated adenine nucleosides showed an increase upon Cd stress in comparison with untreated controls (Supplementary Figure 9.D,E in the Supporting Information). This is in line with the observed up-regulation of adenosine kinase (spot no. 3610 - Table 1, Figure 1B). Deregulation of thiolated purine compounds is suggestive of a likely increase in the metabolic fluxes toward accumulation of thiol-containing compounds, which is confirmed by the Cd-proportional accumulation of homocysteine (Figure 2F) and methionine (data not shown).

TCA Cycle and Glycolysis: Cd Does Not Significantly Promote Accumulation of Carboxylic Acids, While It Promotes Lactate Accumulation. Other than thiol-containing compounds, plants exploit the negative charges of carboxylic groups from organic acids and polycarboxylated compounds to strongly bound heavy metals that are present in the soil and make them soluble and available for plant uptake.[45] While novel low affinity cation transporters have been recently identified in rice (OsLCT1), which might mediate Cd transport in the phloem,[101] in 2007, Wei and colleagues demonstrated that in the xylem sap metal ions are combined to oxygen or nitrogen atoms, indicating that their translocation might involve organic acids or amino acids.[102]

Metal–chelated complexes of organic acids and heavy metals, such Cd–citrate, could be transported more efficiently by transpiration flow from root to the shoot, as observed in tomato,[103] cucumber,[104] and *B. juncea* exposed to lead.[45]

Accumulation of organic acids of the TCA cycle (hereby graphed in Figure 4A–F) has been reported to serve as a strategy to chelate Cd and transport it to the aerial parts of the

dx.doi.org/10.1021/pr400793e | J. Proteome Res. XXXX, XXX, XXX–XXX

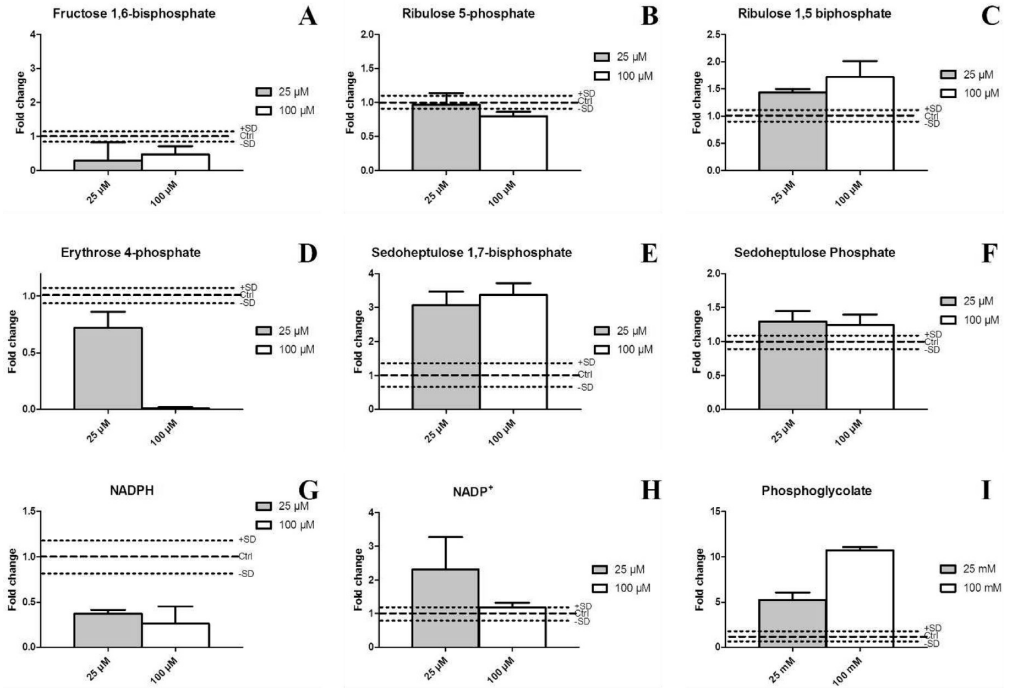

Figure 6. Variation in the levels of metabolic intermediates of the Calvin cycle (A–H) and photorespiration (I) in the leaves of *Brassica juncea* subjected to different Cd concentration normalized against untreated controls (gaped line at one-fold change, ± SD calculated across normalized biological replicates of control leaves). Measurements were performed in triplicate on pooled ground leaves coming from four individual plants per group (control, 25 and 100 μM).

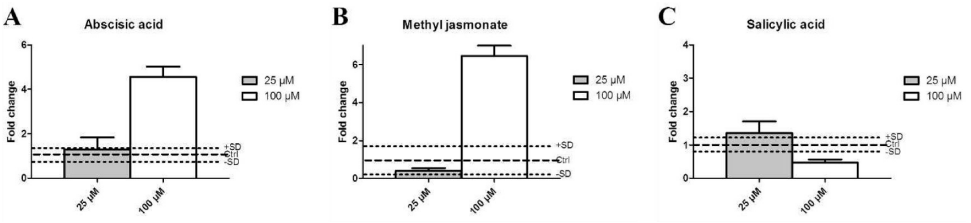

Figure 7. Variation in the levels of plant hormones, abscisic acid (A), methyl jasmonate (B), and salicylic acid (C), in the leaves of *Brassica juncea* subjected to different Cd concentration normalized against untreated controls (gaped line at one-fold change, ± SD calculated across normalized biological replicates of control leaves). Measurements were performed in triplicate on pooled ground leaves coming from four individual plants per group (control, 25 and 100 μM).

plant. This has been shown to be true especially for citrate and malate.[45,103,104] While Cd exposure resulted in a subset of organic acid from the TCA showing higher than control levels (including citrate – Figure 4B, fumarate – Figure 4E, and malate – Figure 4F), this phenomenon was not as evident in the present study in comparison with previous reports from the literature about *B. juncea* responses to lead stress.[45–47] However, it is worthwhile to stress that we assayed leaves instead of roots, while transport in the xylem sap should involve metal–organic acid complexes that, depending on their stability, might have not been not amenable to the analytical approach adopted in the present study.

In the routine metabolic interpretation, organic acids of the TCA cycle are regarded as a substrate to fuel energy production in the mitochondria. Integrating the results from Figure 4 with those related to metabolic intermediates of glycolysis (Figure 3), we could conclude that despite an accumulation of glycolytic intermediates proportionally to Cd concentrations, including hexose phosphate and phosphoenolpyruvate (Figure 5A,C, respectively), utter ATP levels dropped rapidly even under mild Cd stress conditions (Figure 5F). This is also consistent with proteomics results, showing the accumulation of fragments of the chloroplast ATP synthase subunits (Figure 1, Table 1), resulting in the impairment of new ATP synthesis capacity.

Energy metabolism via glycolysis was exacerbated in 25 μM throughout the whole glycolytic pathway. However, in 100 μM Cd, hexose phosphates and phosphoenolpyruvate accumulated without any substantial increase in the levels of lactate, while pyruvate decreased significantly. In other biological systems, this metabolic fingerprint is suggestive of a blockade in early glycolysis toward the pentose phosphate pathway[105–108] (and, in this case, the Calvin cycle), while a blockade at the phosphoenolpyruvate level (Figure 5C) could be suggestive of the up-regulation of amino acid synthesis from a serine backbone.[108,109] This might be the case of cysteine (as confirmed experimentally - Supplementary Figure 10.A in the Supporting Information), which can be produced from a serine backbone (Figure 10.B in the Supporting Information) via cysteine synthase (spot no. 5508 – up-regulated both in 25 and 100 μM Cd leaves – Table 1).

dx.doi.org/10.1021/pr400793e | J. Proteome Res. XXXX, XXX, XXX–XXX

In light of the considerations above, we thus focused on the pentose phosphate pathway and the Calvin cycle to understand whether the blockade in early glycolysis resulted in a metabolic shift toward these pathways.

Calvin cycle was not significantly altered upon Cd exposure (Figure 6). However, integration of proteomics and metabolomics results revealed interesting correlations. For example, in 25 μM samples we could observe a decrease in metabolic substrates (fructose 1,6 biphosphate aldolase − Figure 6A) or accumulation of metabolic products (glyceraldehyde 3-phosphate − Figure 5B) of up-regulated enzymes (fructose 1,6 biphosphate aldolase − spot no. 5508 in Table 1). Analogously, sedoheptulose 1,7 biphosphate accumulation in both mild and heavy Cd stressed leaves (Figure 6F) corresponded to a down-regulation of the enzyme sedoheptulose 1,7-biphosphatase (spot no. 2505 in Table 1). Analogously, alterations to RuBisCO at the protein level (spots nos. 0306, 1701, 1708, 1812, 2702, 2717, 3610, 3812, 6204, 6205, and 7203) resulted in the accumulation of the metabolic substrate ribulose 1,5 biposphate (Figure 6C) proportionally to Cd concentration.

Taken together, the hereby presented proteomics (Table 1) and metabolomics results (Figures 5 and 6) indicate that light-independent carbon fixation reactions and reduced transpiration might be responsible for the Cd-induced depression of the growth rate in the C3 plant *B. juncea* starting from low doses of Cd, while photosystem efficiency was especially affected at 50−100 μM $CdCl_2$ concentrations (Supplementary Table 3 in the Supporting Information). When considering these molecular fingerprints in the light of the deregulated carbon dioxide homeostasis, resulting in the intracellular accumulation of CO_2 (Supplementary Table 1 in the Supporting Information), it is interesting to hypothesize that Cd stress might promote photorespiration so as to prevent photosystem oxidation in response to the drop in stomatal conductance that, under prolonged photosynthesis, would result in CO_2 depletion and O_2 accumulation, thereby triggering oxidative stress phenomena.[110] Therefore, photorespiration could serve as an energy sink preventing the over-reduction of the photosynthetic electron-transport chain and photoinhibition, especially under stress conditions that lead to reduced rates of photosynthetic CO_2 assimilation.[110] Furthermore, photorespiration would provide metabolites for other metabolic processes, for example, glycine for the synthesis of glutathione,[110] which is also involved in stress protection, as detailed above. During photorespiratory metabolism, oxygenation of two molecules of ribulose 1,5-biphosphate generates two molecules of 3-phosphoglycerate and two molecules of phosphoglycolate.[110] In line with these considerations, in the present study, metabolomics analyses suggested that Cd stress might result in the activation of photorespiratory reactions in *B. juncea* because we could observe an evident Cd-dependent increase in the levels of phosphoglycolate (fold-change >5 and 10 in 25 and 100 μM, respectively; Figure 6I).

Cd-Induced Proline Accumulation at the Cross-Road of the above-Listed Metabolic Pathways. In agreement with the literature,[111] metabolomics indicated a Cd-dependent accumulation in the levels of proline (Supplementary Figure 11 in the Supporting Information). Proline has long been known to accumulate in plants experiencing water limitation (as hereby observed − Supplementary Table 1 in the Supporting Information). and this assumption has fueled studies about the use of proline as a beneficial solute allowing plants to increase cellular osmolarity during water limitation.[112] In particular, connections of proline metabolism to redox homeostasis, the oxidative pentose phosphate pathway, and glutamate-glutamine metabolism have been extensively reviewed,[112] also in relation to plant responses to abiotic stresses.[113]

Hormones and *B. juncea* Responses to Cd Stress: Hints from Metabolomics. Plant hormones are known to play a role in plant responses to abiotic stresses, including exposure to heavy metals.[19,20,40,114,115] As it has been recently reviewed,[1] literature reports have shown that virtually all hormonal classes can act as components of Cd-stress signaling, for example, by directly enhancing antioxidant defenses.[114−116] Through metabolomics approaches, in the present study, we could detect and relatively quantify the levels of three main plant hormones in responses to Cd stress (Figure 7). Exposure to high concentrations of Cd promoted abscisic acid (Figure 7A) and methyl jasmonate signaling (Figure 7B), while low dose promoted minor increases in the levels of salicylic acid (Figure 7C). Despite these promising results, further studies are mandatory.

4. CONCLUSIONS

From the present study, it emerges that the hyperaccumulator *B. juncea* responds to Cd stress by accumulating it in the roots and partially translocating it to the shoots. Physiological, proteomics, and metabolomics analyses highlighted that exposure to $CdCl_2$ resulted in the alteration of photosystem efficiency (especially at 50−100 μM), deregulation of ATP synthesis, reduced transpiration, and light-independent carbon fixation reactions. These events are responsible for the depression of plant growth following mild and heavy Cd stress (especially in the latter case).

Taken together, physiological, proteomics, and metabolomics data provided different pieces of the same puzzle that helped us to draw a unified biological interpretation. For example, physiology results highlighted a Cd-induced deregulation of carbon dioxide homeostasis, which resulted in the intracellular accumulation of CO_2. At the same time, proteomics analyses revealed a Cd-dependent alteration of beta carbonic anhydrase. These results were interpreted to hypothesize that Cd stress could result in the promotion of photorespiration, as to prevent photosystem oxidation in response to the drop in stomatal conductance, as gleaned from physiological data. This hypothesis was underpinned by metabolomics results, as we could detect a Cd-dependent accumulation of phosphoglycolate, an indicator of photorespiratory metabolism.

Finally, the application of untargeted metabolomics approaches suggested that plant hormones might also play a nonsecondary role in mediating Cd-stress signaling.

In line with recent trends in the field of Omics technologies, we hereby provide another supportive evidence underpinning the need to increasingly integrate the results from proteomics and metabolomics in the research endeavor dealing with plant abiotic stresses.

■ ASSOCIATED CONTENT

Supporting Information

Supplementary tables and figures and further details of protein identifications. This material is available free of charge via the Internet at http://pubs.acs.org.

dx.doi.org/10.1021/pr400793e | J. Proteome Res. XXXX, XXX, XXX−XXX

AUTHOR INFORMATION

Corresponding Authors

*Tel: +39 0761 357 100. Fax: +39 0761 357 179. E-mail: zolla@unitus.it (L.Z.).
*E-mail: tahar.ghnaya@gmail.com (T.G.).

Author Contributions

§A.D. and M.T. contributed equally and share the first authorship.

Notes

The authors declare no competing financial interest.

ACKNOWLEDGMENTS

Seeds of *B. juncea* (Acc 426308) were kindly provided by the North Central Regional Plant Introduction Station (NCRPIS), United States Department of Agriculture (USDA) from United States of America.

L.Z. and A.D.A. are supported by mobility studentship funds and a postdoctoral research grant by the Interuniversity Consortium for Biotechnologies (CIB).

REFERENCES

(1) Azevedo, R. A.; Gratão, P. L.; Monteiro, C. C.; Carvalho, R. F. What is new in the research on cadmium-induced stress in plants? *Food. Energy Secur.* **2012**, *1* (2), 133−140.

(2) Zawoznik, M. S.; Groppa, M. D.; Tomaro, M. L.; Benavides, M. P. Endogenous salicylic acid potentiates cadmium-induced oxidative stress in *Arabidopsis thaliana*. *Plant Sci.* **2007**, *173*, 190−197.

(3) Buchet Järup, L.; Akesson, A. Current status of cadmium as an environmental health problem. *Toxicol. Appl. Pharmacol.* **2009**, *238* (3), 201−208.

(4) DalCorso, G.; Farinati, S.; Furini, A. Regulatory networks of cadmium stress in plants. *Plant Signal. Behav.* **2010**, *5* (6), 663−667.

(5) D'Alessandro, A.; Zolla, L. We are what we eat: food safety and proteomics. *J. Proteome Res.* **2012**, *11* (1), 26−36.

(6) Fagioni, M.; D'Amici, G. M.; Timperio, A. M.; Zolla, L. Proteomic analysis of multiprotein complexes in the thylakoid membrane upon cadmium treatment. *J. Proteome Res.* **2009**, *8* (1), 310−326.

(7) Gallego, S. M.; Pena, L. B.; Barcia, R. A.; Azpilicueta, C. E.; Lannone, M. F.; Rosales, E. P.; Zawoznik, M. S.; Groppa, M. D.; Benavides, M. P. Unravelling cadmium toxicity and tolerance in plants: insight into regulatory mechanisms. *Environ. Exp. Bot.* **2012**, *83*, 33−46.

(8) Sanità di Toppi, L.; Gabbrielli, R. Response to cadmium in higher plants. *Environ. Exp. Bot.* **1999**, *41*, 105−130.

(9) Benavides, M. P.; Gallego, S. M.; Tomaro, M. L. Cadmium toxicity in plants. *Braz. J. Plant Physiol.* **2005**, *17*, 21−34.

(10) Polle, A.; Schuetzenduebel, A. Heavy Metal Signalling in Plants: Linking Cellular and Organismic Responses. In *Plant Responses to Abiotic Stress*; Hirt, H., Shinozaki, K., Eds.; Springer-Verlag: Berlin-Heidelberg, 2003; pp 187−215.

(11) Maksymiec, W. Signaling responses in plants to heavy metal stress. *Acta Physiol. Plant.* **2007**, *29*, 177−187.

(12) Mithoefer, A.; Schulze, B.; Boland, W. Biotic and heavy metal stress response in plants: evidence for common signals. *FEBS Lett.* **2004**, *566*, 1−5.

(13) Qureshi, M. I.; D'Amici, G. M.; Fagioni, M.; Rinalducci, S.; Zolla, L. Iron stabilizes thylakoid protein-pigment complexes in Indian mustard during Cd-phytoremediation as revealed by BN-SDS-PAGE and ESI-MS/MS. *J. Plant Physiol.* **2010**, *167* (10), 761−770.

(14) Fagioni, M.; Zolla, L. Does the different proteomic profile found in apical and basal leaves of spinach reveal a strategy of this plant toward cadmium pollution response? *J. Proteome Res.* **2009**, *8* (5), 2519−2529.

(15) Tian, S. K.; Lu, L. L.; Yang, X. E.; Huang, H. G.; Wang, K.; Brown, P. H. Root adaptations to cadmium-induced oxidative stress contribute to Cd tolerance in the hyperaccumulator *Sedum alfredii*. *Biol. Plant.* **2012**, *56*, 344−350.

(16) Clemens, S. Evolution and function of phytochelatin synthases. *J. Plant Physiol.* **2006**, *163*, 319−332.

(17) Cobbett, C. S. Phytochelatins and their roles in heavy metal detoxification. *Plant Physiol.* **2000**, *123*, 825−832.

(18) Noriega, G.; Santa Cruz, D.; Batlle, A.; Tomaro, M.; Balestrasse, K. Heme oxygenase is involved in the protection exerted by jasmonic acid against cadmium stress in soybean roots. *J. Plant Growth Regul.* **2012**, *31*, 79−89.

(19) Monteiro, C. C.; Carvalho, R. F.; Gratão, P. L.; Carvalho, G.; Tezotto, T.; Medici, L. O.; Peres, L. E. P.; Azevedo, R. A. Biochemical responses of the ethylene-insensitive Never ripe tomato mutant subjected to cadmium and sodium stresses. *Environ. Exp. Bot.* **2011**, *71*, 306−320.

(20) Gratão, P. L.; Monteiro, C. C.; Carvalho, R. F.; Tezotto, T.; Piotto, F. A.; Peres, L. E. P.; Azevedo, R. A. Biochemical dissection of diageotropica and Never ripe tomato mutants to Cd stressful conditions. *Plant Physiol. Biochem.* **2012**, *56*, 79−96.

(21) Baker, A. J. M.; McGrath, S. P.; Reeves, R. D.; Smith, J. A. C. Metal Hyperaccumulator Plants: A Review of the Ecology and Physiology of a Biological Resource for Phytoremediation of Metal-Polluted Soils. In *Phytoremediation of Contaminated Soil and Water*; Terry, N., Bañuelos, G., Eds.; Lewis Publisher, Boca Raton, FL, 2000; pp 85−107.

(22) Bhargava, A.; Carmona, F. F.; Bhargava, M.; Srivastava, S. Approaches for enhanced phytoextraction of heavy metals. *J. Environ Manage.* **2012**, *105*, 103−120.

(23) Shanmugaraj, B. M.; Chandra, H. M.; Srinivasan, B.; Ramalingam, S. Cadmium induced physio-biochemical and molecular response in *Brassica juncea*. *Int. J. Phytorem.* **2013**, *15* (3), 206−218.

(24) Bauddh, K.; Singh, R. P. Cadmium tolerance and its phytoremediation by two oil yielding plants *Ricinus communis* (L.) and *Brassica juncea* (L.) from the contaminated soil. *Int. J. Phytorem.* **2012**, *14* (8), 772−785.

(25) Mohamed, A. A.; Castagna, A.; Ranieri, A.; Sanità di Toppi, L. Cadmium tolerance in *Brassica juncea* roots and shoots is affected by antioxidant status and phytochelatin biosynthesis. *Plant Physiol. Biochem.* **2012**, *57*, 15−22.

(26) Song, W. Y.; Choi, K. S.; Alexis de, A.; Martinoia, E.; Lee, Y. *Brassica juncea* plant cadmium resistance 1 protein (BjPCR1) facilitates the radial transport of calcium in the root. *Proc. Natl. Acad. Sci. U.S.A.* **2011**, *108* (49), 19808−19813.

(27) Masood, A.; Iqbal, N.; Khan, N. A. Role of ethylene in alleviation of cadmium-induced photosynthetic capacity inhibition by sulphur in mustard. *Plant Cell Environ.* **2012**, *35* (3), 524−533.

(28) Gill, S. S.; Khan, N. A.; Tuteja, N. Differential cadmium stress tolerance in five indian mustard (*Brassica juncea* L.) cultivars: an evaluation of the role of antioxidant machinery. *Plant Signal. Behav.* **2011**, *6* (2), 293−300.

(29) Lang, M.; Hao, M.; Fan, Q.; Wang, W.; Mo, S.; Zhao, W.; Zhou, J. Functional characterization of BjCET3 and BjCET4, two new cation-efflux transporters from *Brassica juncea* L. *J. Exp. Bot.* **2011**, *62* (13), 4467−4480.

(30) Farinati, S.; DalCorso, G.; Varotto, S.; Furini, A. The *Brassica juncea* BjCdR15, an ortholog of Arabidopsis TGA3, is a regulator of cadmium uptake, transport and accumulation in shoots and confers cadmium tolerance in transgenic plants. *New Phytol.* **2010**, *185* (4), 964−978.

(31) Alvarez, S.; Berla, B. M.; Sheffield, J.; Cahoon, R. E.; Jez, J. M.; Hicks, L. M. Comprehensive analysis of the *Brassica juncea* root proteome in response to cadmium exposure by complementary proteomic approaches. *Proteomics* **2009**, *9* (9), 2419−2431.

(32) Verma, K.; Shekhawat, G. S.; Sharma, A.; Mehta, S. K.; Sharma, V. Cadmium induced oxidative stress and changes in soluble and ionically bound cell wall peroxidase activities in roots of seedling and

3−4 leaf stage plants of *Brassica juncea* (L.) czern. *Plant Cell Rep.* **2008**, *27* (7), 1261−1269.
(33) Seth, C. S.; Kumar Chaturvedi, P.; Misra, V. The role of phytochelatins and antioxidants in tolerance to Cd accumulation in *Brassica juncea* L. *Ectoxicol. Environ. Saf.* **2008**, *71* (1), 76−85.
(34) Van Engelen, D. L.; Sharpe-Pedler, R. C.; Moorhead, K. K. Effect of chelating agents and solubility of cadmium complexes on uptake from soil by *Brassica juncea*. *Chemosphere.* **2007**, *68* (3), 401−408.
(35) Jiang, X. J.; Luo, Y. M.; Liu, Q.; Liu, S. L.; Zhao, Q. G. Effects of cadmium on nutrient uptake and translocation by Indian Mustard. *Environ. Geochem. Health* **2004**, *26* (2−3), 319−324.
(36) Su, D. C.; Wong, J. W. Selection of mustard oilseed rape (*Brassica juncea* L.) for phytoremediation of cadmium contaminated soil. *Bull. Environ. Contam. Toxicol.* **2004**, *72* (5), 991−998.
(37) Crist, R. H.; Martin, J. R.; Crist, D. R. Ion-exchange aspects of toxic metal uptake by Indian mustard. *Int. J. Phytorem.* **2004**, *6* (1), 85−94.
(38) Mendoza, J.; Soto, P.; Ahumada, I.; Garrido, T. Determination of oxidized and reduced glutathione, by capillary zone electrophoresis, in *Brassica juncea* plants treated with copper and cadmium. *Electrophoresis* **2004**, *25* (6), 890−896.
(39) Heiss, S.; Wachter, A.; Bogs, J.; Cobbett, C.; Rausch, T. Phytochelatin synthase (PCS) protein is induced in *Brassica juncea* leaves after prolonged Cd exposure. *J. Exp. Bot.* **2003**, *54* (389), 1833−1839.
(40) Salt, D. E.; Prince, R. C.; Pickering, I. J.; Raskin, I. Mechanisms of Cadmium Mobility and Accumulation in Indian Mustard. *Plant Physiol.* **1995**, *109* (4), 1427−1433.
(41) Speiser, D. M.; Abrahamson, S. L.; Banuelos, G.; Ow, D. W. *Brassica juncea* Produces a Phytochelatin-Cadmium-Sulfide Complex. *Plant Physiol.* **1992**, *99* (3), 817−821.
(42) Hossain, Z.; Komatsu, S. Contribution of proteomic studies towards understanding plant heavy metal stress response. *Front. Plant Sci.* **2012**, *3*, 310.
(43) Urano, K.; Kurihara, Y.; Seki, M.; Shinozaki, K. 'Omics' analyses of regulatory networks in plant abiotic stress responses. *Curr. Opin. Plant Biol.* **2010**, *13*, 1−7.
(44) Villiers, F.; Ducruix, C.; Hugouvieux, V.; Jarno, N.; Ezan, E.; Garin, J.; Junot, C.; Bourguignon, J. Investigating the plant response to cadmium exposure by proteomic and metabolomic approaches. *Proteomics* **2011**, *11* (9), 1650−1663.
(45) Ghnaya, T.; Zaier, H.; Baioui, R.; Sghaier, S.; Lucchini, G.; Sacchi, G. A.; Lutts, S.; Abdelly, C. Implication of organic acids in the long-distance transport and the accumulation of lead in *Sesuvium portulacastrum* and *Brassica juncea*. *Chemosphere.* **2013**, *90* (4), 1449−1454.
(46) Aldrich, M. V.; Gardea-Torresdey, J. L.; Peralta-Videa, J. R.; Parsons, J. G. Uptake and reduction of Cr (VI) to Cr (III) by mesquite (Prospis spp.): chromate-plant interaction in hydroponics and solid media studied using XAS. *Environ. Sci. Technol.* **2003**, *37*, 1859−1864.
(47) Schurr, U. Xylem sap sampling − new approaches to an old topic. *Trends Plant Sci.* **1999**, *3*, 293−298.
(48) Shevchenko, A.; Wilm, M.; Vorm, O.; Mann, M. Mass spectrometric sequencing of proteins silver-stained polyacrylamide gels. *Anal. Chem.* **1996**, *68*, 850−858.
(49) D'Alessandro, A.; Rinalducci, S.; Marrocco, C.; Zolla, V.; Napolitano, F.; Zolla, L. Love me tender: an Omics window on the bovine meat tenderness network. *J. Proteomics* **2012**, *75* (14), 4360−4380.
(50) D'Alessandro, A.; Marrocco, C.; Rinalducci, S.; Peschiaroli, A.; Timperio, A. M.; Bongiorno-Borbone, L.; Finazzi Agrò, A.; Melino, G.; Zolla, L. Analysis of TAp73-Dependent Signaling via Omics Technologies. *J. Proteome Res.* **2013**, *12*, 4207−4220.
(51) D'Alessandro, A.; Gevi, F.; Zolla, L. A robust high resolution reversed-phase HPLC strategy to investigate various metabolic species in different biological models. *Mol. Biosyst.* **2011**, *7* (4), 1024−1032.
(52) D'Alessandro, A.; Gevi, F.; Zolla, L. Red blood cell metabolism under prolonged anaerobic storage. *Mol. Biosyst.* **2013**, *9* (6), 1196−1209.
(53) Melamud, E.; Vastag, L.; Rabinowitz, J. D. Metabolomic analysis and visualization engine for LC-MS data. *Anal. Chem.* **2010**, *82* (23), 9818−9826.
(54) Kanehisa, M.; Goto, S. KEGG: kyoto encyclopedia of genes and genomes. *Nucleic Acids Res.* **2000**, *28* (1), 27−30.
(55) Wan, G.; Najeeb, U.; Jilani, G.; Naeem, M. S.; Zhou, W. Calcium invigorates the cadmium-stressed *Brassica napus* L. plants by strengthening their photosynthetic system. *Environ. Sci. Pollut Res.* **2011**, *18* (9), 1478−1486.
(56) Cheung, W. Y. Calmodulin: its potential role in cell proliferation and heavy metal toxicity. *Fed. Proc.* **1984**, *43*, 2995−2999.
(57) Perfus-Barbeoch, L.; Leonhardt, N.; Vavaddeur, A.; Forestier, C. Heavy metal toxicity: cadmium permeates through calcium channels and disturbs the plant water status. *Plant J.* **2002**, *32*, 539−548.
(58) Yang, T.; Poovaiah, B. W. Calcium/calmodulin-mediated signal network in plants. *Trends. Plant Sci.* **2003**, *8*, 505−512.
(59) Arazi, T.; Kaplan, B.; Sunkar, R.; Fromm, H. Cyclic-nucleotide- and Ca^{2+}/calmodulin-regulated channels in plants: targets for manipulating heavy-metal tolerance, and possible physiological roles. *Biochem. Soc. Trans.* **2000**, *28*, 471−475.
(60) Zhu, L. Y.; Pilon-Smits, E. A. H.; Jouanin, L.; Terry, N. Overexpression of Glutathione Synthetase in Indian Mustard Enhances Cadmium Accumulation and Tolerance. *Plant Physiol.* **1999**, *119* (1), 73−80.
(61) Haag-Kerwer, A.; Schafer, H. J.; Heiss, S.; Walter, C.; Rausch, T. Cadmium exposure in *Brassica juncea* causes a decline in transpiration rate and leaf expansion without effect on photosynthesis. *J. Exp. Bot.* **1999**, *50* (341), 1827−1835.
(62) Vrettos, J. S.; Stone, D. A.; Brudvig, G. W. Quantifying the ion selectivity of the Ca2+ site in photosystem II: evidence for direct involvement of Ca2+ in O2 formation. *Biochemistry* **2001**, *40*, 7937−7945.
(63) Ebbs, S.; Uchil, S. Cadmium and zinc induced chlorosis in Indian mustard [Brassica juncea (L.) Czern] involves preferential loss of chlorophyll b. *Photosynthetica* **2008**, *46* (1), 49−55.
(64) DalCorso, G.; Farinati, S.; Maistri, S.; Furini, A. How plants cope with cadmium: staking all on metabolism and gene expression. *J. Integr. Plant Biol.* **2008**, *50*, 1268−1280.
(65) Fusco, N.; Micheletto, L.; Dal Corso, G.; Borgato, L.; Furini, A. Identification of cadmium-regulated genes by cDNA-AFLP in the heavy metal accumulator *Brassica juncea* L. *J. Exp. Bot.* **2005**, *56* (421), 3017−3027.
(66) Weber, M.; Trampczynska, A.; Clemens, S. Comparative transcriptome analysis of toxic metal responses in *Arabidopsis thaliana* and the Cd^{2+}-hypertolerant facultative metallophyte *Arabidopsis halleri*. *Plant Cell. Environ.* **2006**, *29*, 950−963.
(67) Lin, Y. F.; Aarts, M. G. M. The molecular mechanism of zinc and cadmium stress response in plants. *Cell. Mol. Life Sci.* **2012**, *69*, 3187−3206.
(68) Verbruggen, N.; Hermans, C.; Schat, H. Mechanisms to cope with arsenic or cadmium excess in plants. *Curr. Opin. Plant Biol.* **2009**, *12*, 1−9.
(69) Wang, Z.; Zhang, Y.; Huang, Z.; Huang, L. Antioxidative response of metal-accumulator and non-accumulator plants under cadmium stress. *Plant Soil* **2008**, *310*, 137−149.
(70) Romero-Puertas, M. C.; Corpas, F. J.; Rodriguez-Serrano, M.; Gomez, M.; del Rio, L. A.; Sandalio, L. M. Differential expression and regulation of antioxidative enzymes by cadmium in pea plants. *J. Plant Physiol.* **2007**, *164*, 1346−1357.
(71) Dat, J. F.; Vandenabeele, S.; Vranova, E.; Van Montagu, M.; Inze, D.; Van Breusegem, F. Dual action of the active oxygen species during plant stress responses. *Cell. Mol. Life Sci.* **2000**, *57*, 779−795.
(72) Schützendübel, A.; Polle, A. Plant responses to abiotic stresses: heavy metal-induced oxidative stress and protection by mycorrhization. *J. Exp. Bot.* **2002**, *53* (372), 1351−1365.

(73) Siedlecka, A.; Gardestrom, P.; Samuelsson, G.; Kleczkowski, L. A.; Krupa, Z. A relationship between carbonic anhydrase and rubisco in response to moderate cadmium stress during light activation of photosynthesis. *J. Biosci.* **1999**, *54*, 759−776.
(74) Ying, R. R.; Qiu, R. L.; Tang, Y. T.; Hu, P. J.; Qiu, H.; Chen, H. R.; Shi, T. H.; Morel, J. L. Cadmium tolerance of carbon assimilation enzymes and chloroplast in Zn/Cd hyperaccumulator *Picris divaricata*. *J. Plant Physiol.* **2010**, *167* (2), 81−87.
(75) Seo, J.; Kong-Joo, L. Post-translational Modifications and Their Biological Functions: Proteomic Analysis and Systematic Approaches. *J. Biochem. Mol. Biol.* **2004**, *37* (1), 35−44.
(76) D'Alessandro, A.; Marrocco, C.; Rinalducci, S.; Mirasole, C.; Failla, S.; Zolla, L. Chianina beef tenderness investigated through integrated Omics. *J Proteomics* **2012**, *75* (14), 4381−4398.
(77) D'Alessandro, A.; Rinalducci, S.; Marrocco, C.; Zolla, V.; Napolitano, F.; Zolla, L. Love me tender: an Omics window on the bovine meat tenderness network. *J. Proteomics* **2012**, *75* (14), 4360−4380.
(78) Langenkämper, G.; Manac'h, N.; Broin, M.; Cuiné, S.; Becuwe, N.; Kuntz, M.; Rey, P. Accumulation of plastid lipid-associated proteins (fibrillin/CDSP34) upon oxidative stress, ageing and biotic stress in Solanaceae and in response to drought in other species. *J. Exp. Bot.* **2001**, *52* (360), 1545−1554.
(79) Timperio, A. M.; Egidi, M. G.; Zolla, L. Proteomics applied on plant abiotic stresses: role of heat shock proteins (HSP). *J. Proteomics* **2008**, *71* (4), 391−411.
(80) Rodríguez-Serrano, M.; Romero-Puertas, M. C.; Pazmiño, D. M.; Testillano, P. S.; Risueño, M. C.; Del Río, L. A.; Sandalio, L. M. Cellular response of pea plants to cadmium toxicity: cross talk between reactive oxygen species, nitric oxide, and calcium. *Plant Physiol.* **2009**, *150* (1), 229−243.
(81) Sandalio, L. M.; Rodríguez-Serrano, M.; Gupta, D. K.; Archilla, A.; Romero-Puertas, M. C.; Río, L. A. Reactive Oxygen Species and Nitric Oxide in Plants under Cadmium Stress: From Toxicity to Signaling. In *Environmental Adaptations and Stress Tolerance of Plants in the Era of Climate Change*; Springer: New York, 2012; pp 199−215.
(82) Schaeffer, H. J.; Weber, M. J. Mitogen-activated protein kinases: specific messages from ubiquitous messengers. *Mol. Cell. Biol.* **1999**, *19*, 2435−2444.
(83) Jonak, C.; Nakagami, H.; Hirt, H. Heavy metal stress. Activation of distinct mitogen-activated protein kinase pathways by copper and cadmium. *Plant Physiol.* **2004**, *136*, 3276−3283.
(84) Lundin, B.; Hansson, M.; Schoefs, B.; Vener, A. V.; Spetea, C. The Arabidopsis $PsbO_2$ protein regulates dephosphorylation and turnover of the photosystem II reaction centre D1 protein. *Plant J.* **2007**, *49* (3), 528−539.
(85) Wang, Y.; Hu, H.; Zhu, L. Y.; Li, X. X. Response to nickel in the proteome of the metal accumulator plant *Brassica juncea*. *J. Plant Interact.* **2011**, *7* (3), 230−237.
(86) Hossain, Z.; Hajik, M.; Komatsu, S. Comparative proteome analysis of high and low cadmium accumulating soybeans under cadium stress. *Amino Acids* **2012**, *43*, 2393−2416.
(87) Kwinta, J.; Kolilk, D. Glutamine synthetase and glutamate dehydrogenase in cadmium-stressed triticale seedlings. *Acta Physiol. Plant.* **2006**, *28* (4), 339−347.
(88) Kralova, K.; Jampilek, J.; Ostrovsky, I. Metabolomics − Useful tool for study of plant responses to abiotic stresses. *Ecol. Chem. Eng. S.* **2012**, *19* (2), 133−161.
(89) Nocito, F. F.; Lancilli, C.; Giacomini, B.; Sacchi, G. A. Sulfur Metabolism and Cadmium Stress in Higher Plants. *Plant Stress* **2007**, *1* (2), 142−156.
(90) Gill, S. S.; Tuteja, N. Cadmium stress tolerance in crop plants: probing the role of sulfur. *Plant Signal. Behav.* **2011**, *6* (2), 215−222.
(91) Ernst, W. H.; Krauss, G. J.; Verkleij, J. A. C.; Wesemberg, D. Interaction of heavy metals with the sulphur metabolism in angiosperms from an ecological point of view. *Plant Cell Environ.* **2008**, *31*, 123−143.
(92) Van de Mortel, J. E.; Schat, H.; Moerland, P. D.; Ver Loren van Themaat, E.; van der Ent, S.; Blankestijn, H.; Ghandilyan, A.; Tsiatsiani, S.; Aarts, M. G. Expression differences for genes involved in lignin, glutathione and sulphate metabolism in response to cadmium in *Arabidopsis thaliana* and the related Zn/Cd-hyperaccumulator *Thlaspi caerulescens*. *Plant Cell Environ.* **2008**, *31*, 301−324.
(93) Ahsan, N.; Nakamura, T.; Komatsu, S. Differential responses of microsomal proteins and metabolites in two contrasting cadmium (Cd)-accumulating soybean cultivars under Cd stress. *Amino Acids* **2012**, *42* (1), 317−327.
(94) Nikiforova, V. J.; Kopka, J.; Tolstikov, V.; Fiehn, O.; Hopkins, L.; Hawkesford, M. J.; Hesse, H.; Hoefgen, R. Systems rebalancing of metabolism in response to sulfur deprivation, as revealed by metabolome analysis of Arabidopsis plants. *Plant Physiol.* **2005**, *138* (1), 304−318.
(95) Wang, H. C.; Wu, J. S.; Chia, J. C.; Yang, C. C.; Wu, Y. J.; Juang, R. H. Phytochelatin synthase is regulated by protein phosphorylation at a threonine residue near its catalytic site. *J. Agric. Food. Chem.* **2009**, *57*, 7348−7355.
(96) Heiss, S.; Wachter, A.; Bogs, J.; Cobbett, C.; Rausch, T. Phytochelatin synthase (PCS) protein is induced in *Brassica juncea* leaves after prolonged Cd exposure. *J. Exp. Bot.* **2003**, *54*, 1833−1839.
(97) Yen, T. Y.; Villa, J. A.; DeWitt, J. G. Analysis of Phytochelatin−Cadmium Complexes from Plant Tissue Culture Using Nano-electrospray Ionization Tandem Mass Spectrometry and Capillary Liquid Chromatography/Electrospray Ionization Tandem Mass Spectrometry. *J. Mass Spectrom.* **1999**, *34*, 930−941.
(98) Stasolla, C.; Katahira, R.; Thorpe, T. A.; Ashihara, H. Purine and pyrimide nucleotide metabolism in higher plants. *J. Plant Physiol.* **2003**, *160* (11), 1271−1295.
(99) Speiser, D. M.; Ortiz, D. F.; Kreppel, L.; Scheel, G.; McDonald, G.; Ow, D. W. Purine biosynthetic genes are required for cadmium tolerance in *Schizosaccharomyces pombe*. *Mol. Cell. Biol.* **1992**, *12* (12), 5301−5310.
(100) Juang, R. H.; McCue, K. F.; Ow, D. W. Two purine biosynthetic enzymes that are required for cadmium tolerance in *Schizosaccharomyces pombe* utilize cysteine sulfinate in vitro. *Arch. Biochem. Biophys.* **1993**, *304* (2), 392−401.
(101) Uraguchi, S.; Kamiya, T.; Sakamoto, T.; Kasai, K.; Sato, Y.; Nagamura, Y.; Yoshida, A.; Kyozuka, J.; Ishikawa, S.; Fujiwara, T. Low-affinity cation transporter (OsLCT1) regulates cadmium transport into rice grains. *Proc. Natl. Acad. Sci. U. S. A.* **2011**, *108* (52), 20959−20964.
(102) Wei, Z. G.; Wong, J. W.; Zhao, H. Y.; Zhang, H. J.; Li, H. X.; Hu, F. Determination of inorganic and organic anions in xylem saps of two contrasting oilseed rape (*Brassica juncea* L.) varieties: roles of anions in long-distance transport of cadmium. *Microchem. J.* **2007**, *86*, 53−59.
(103) Senden, M. H. M. N.; Van Paassen, F. J. M.; Van Der Mer, A. J. G. M.; Wolterbeek, H. T. H. Cadmium−citric acid−xylem interaction in tomato plants. *Plant Cell Environ.* **1992**, *15*, 71−79.
(104) Tatár, E.; Mihucz, V. G.; Varga, A.; Zaray, G.; Cseh, E. Effect of lead, nickel and vanadium contamination on organic acid transport in xylem sap of cucumber. *J. Inorg. Biochem.* **1999**, *75*, 219−223.
(105) Polati, R.; Castagna, A.; Bossi, A. M.; Alberio, T.; De Domenico, I.; Kaplan, J.; Timperio, A. M.; Zolla, L.; Gevi, F.; D'Alessandro, A.; Brunch, R.; Olivieri, O.; Girelli, D. Murine macrophages response to iron. *J. Proteomics* **2012**, *76*, 10−27.
(106) Gevi, F.; D'Alessandro, A.; Rinalducci, S.; Zolla, L. Alterations of red blood cell metabolome during cold liquid storage of erythrocyte concentrates in CPD-SAGM. *J. Proteomics* **2012**, *76*, 168−80.
(107) D'Alessandro, A.; D'Amici, G. M.; Timperio, A. M.; Merendino, N.; Zolla, L. Docosohaexanoic acid-supplemented PACA44 cell lines and over-activation of Krebs cycle: an integrated proteomic, metabolomic and interactomic overview. *J. Proteomics* **2011**, *74* (10), 2138−2158.
(108) Maddocks, O. D.; Berkers, C. R.; Mason, S. M.; Zheng, L.; Blyth, K.; Gottlieb, E.; Vousden, K. H. Serine starvation induces stress and p53-dependent metabolic remodelling in cancer cells. *Nature* **2013**, *493* (7433), 542−546.

(109) Chaneton, B.; Hillmann, P.; Zheng, L.; Martin, A. C.; Maddocks, O. D.; Chokkathukalam, A.; Coyle, J. E.; Jankevics, A.; Holding, F. P.; Vousden, K. H.; Frezza, C.; O'Reilly, M.; Gottlieb, E. Serine is a natural ligand and allosteric activator of pyruvate kinase M2. *Nature* **2012**, *491* (7424), 458−462.
(110) Wingler, A.; Lea, P. J.; Quick, W. P.; Leegood, R. C. Photorespiration: metabolic pathways and their role in stress protection. *Philos. Trans. R. Soc., B* **2000**, *355*, 1517−1529.
(111) Dhir, B.; Sharmila, P.; Saradhi, P. P. Hydrophytes lack potential to exhibit cadmium stress induced enhancement in lipid peroxidation and accumulation of proline. *Aquat. Toxicol.* **2004**, *66* (2), 141−147.
(112) Verslues, P. E.; Sharma, S. Proline metabolism and its implications for plant-environment interaction. *Arabidopsis Book*. **2010**, *8*, e0140.
(113) Sharma, S. S.; Dietz, K. J. The relationship between metal toxicity and cellular redox imbalance. *Trends Plant Sci.* **2009**, *14*, 43−50.
(114) Zawoznik, M. S.; Groppa, M. D.; Tomaro, M. L.; Benavides, M. P. Endogenous salicylic acid potentiates cadmium-induced oxidative stress in *Arabidopsis thaliana*. *Plant Sci.* **2007**, *173* (2), 190−197.
(115) Guo, B.; Liang, Y.; Zhu, Y. Does salicylic acid regulate antioxidant defense system, cell death, cadmium uptake and partitioning to acquire cadmium tolerance in rice? *J. Plant Physiol.* **2009**, *166* (1), 20−31.
(116) Stroinski, A.; Gizewska, K.; Zielezinska, M. Abscisic acid is required in transduction of cadmium signal to potato roots. *Biol. Plant.* **2013**, *57* (1), 121−127.